

# Analog quantum simulation of bosonic lattices and lattice gauge theories

**Zheng Shi**

Jamal Busnaina, Dmytro Dubyna, Cindy Yang,  
Ibrahim Nsanzineza, Jimmy Hung, Sandbo Chang, **Chris Wilson**

Alexander McDonald, Jesús Alcaine-Cuervo, Aashish Clerk, Enrique Rico



# “Analog computation actually stimulates creativity.”

*“desk top analog computers... for the ultimate high-speed, low-cost problem solving capabilities”*

## Analog Simulation . . .

Analog Simulation is a dynamic method of solving the problems that confront the engineer and scientist daily — and EAI TR-20 and TR-48 Analog Computers provide an unsurpassed capability for simulating systems of all types. Analog computers help slash project costs by saving time and cost of materials in trial and error testing of prototypes or pilot plants. One engineer with a desk-top PACE® computer can be the equal of several men limited to conventional design tools; moreover, he can gain a unique insight of the dynamic performance of systems to produce a superior product.

Experimentation time and costs are similarly slashed. Ideas that were once too costly or time consuming to be tried can be “debugged” right on the computer. Analog computation actually stimulates creativity.

EAI TR-20 & TR-48 Brochure, 1964

Analog quantum simulation of bosonic lattices and lattice gauge theories

2



# Analog quantum simulation

- Build a **quantum** device with the same dynamics as the system of interest, and measure its time evolution

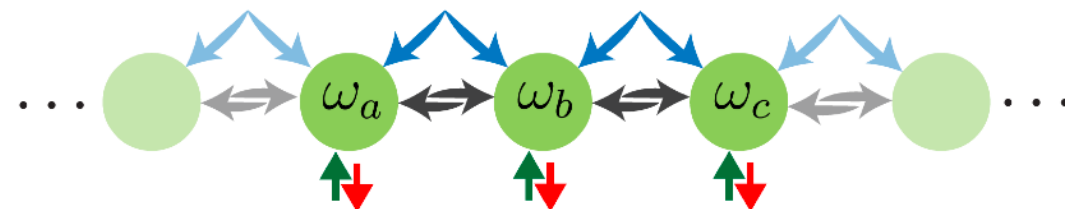
# Analog quantum simulation

- Build a **quantum** device with the same dynamics as the system of interest, and measure its time evolution
- Compared to digital quantum simulation:
  - More specialized hardware – milder hardware requirements
  - Naturally suited to many-body problems (no circuit mapping)
  - No error correction
  - **Practical quantum advantage still possible!**

Cirac & Zoller, Nat. Phys. 8, 264 (2012)  
Trivedi, Rubio & Cirac, Nat. Commun. 15, 6507 (2024)

# This talk

- Analog quantum simulation of bosonic lattice models
  - Bosonic Kitaev chain

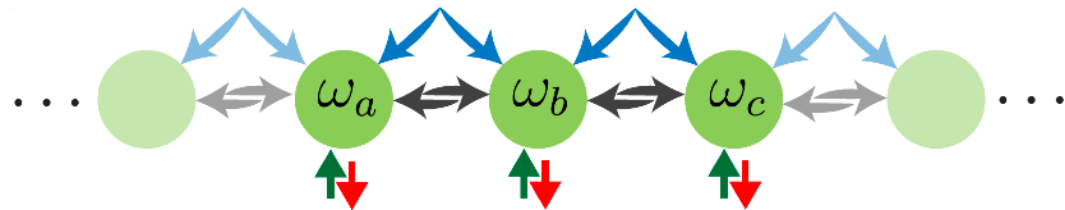


- Analog quantum simulation of lattice gauge theories
  - Three-qubit interaction



# ANALOG QUANTUM SIMULATION OF BOSONIC LATTICE MODELS

Busnaina, ZS, McDonald, Dubyna, Nsanzineza, Hung, Chang, Clerk & Wilson,  
Nat. Commun. 15, 3065 (2024)

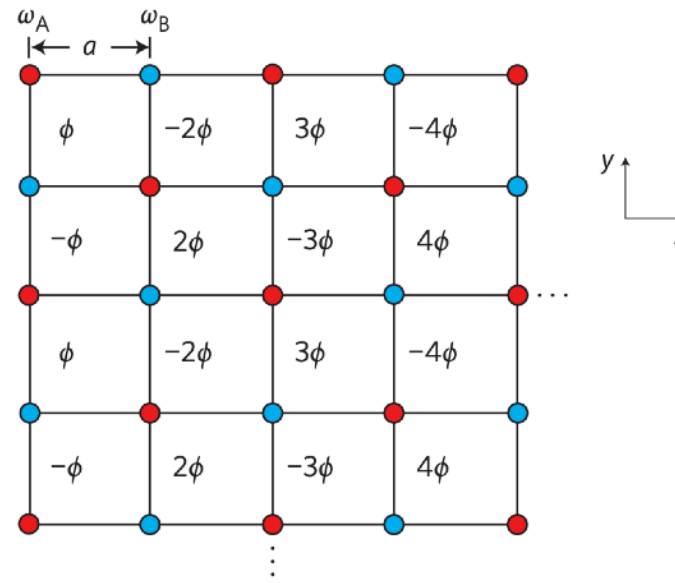


# Background: photonic lattices

Realizing effective magnetic field for photons by controlling the phase of dynamic modulation

Kejie Fang<sup>1</sup>, Zongfu Yu<sup>2</sup> and Shanhui Fan<sup>2\*</sup>

$$\int_i^j \mathbf{A}_{\text{eff}} \cdot d\mathbf{l} = \phi_{ij}$$



- Complex hopping terms with controllable phases

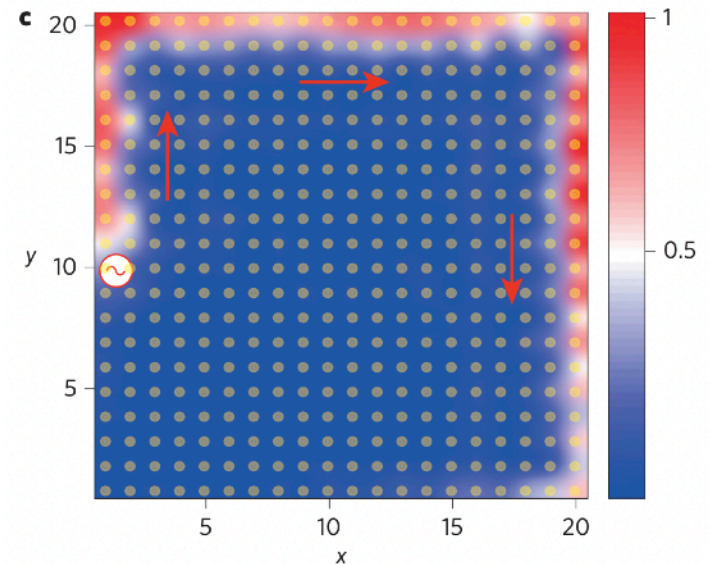
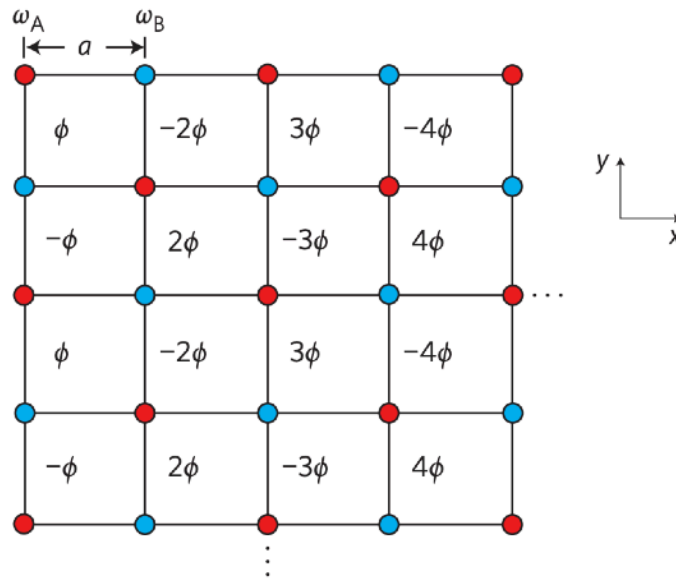
Fang, Yu & Fan, Nat. Photonics 6, 782 (2012)

# Background: photonic lattices

Realizing effective magnetic field for photons by controlling the phase of dynamic modulation

Kejie Fang<sup>1</sup>, Zongfu Yu<sup>2</sup> and Shanhui Fan<sup>2\*</sup>

$$\int_i^j \mathbf{A}_{\text{eff}} \cdot d\mathbf{l} = \phi_{ij}$$

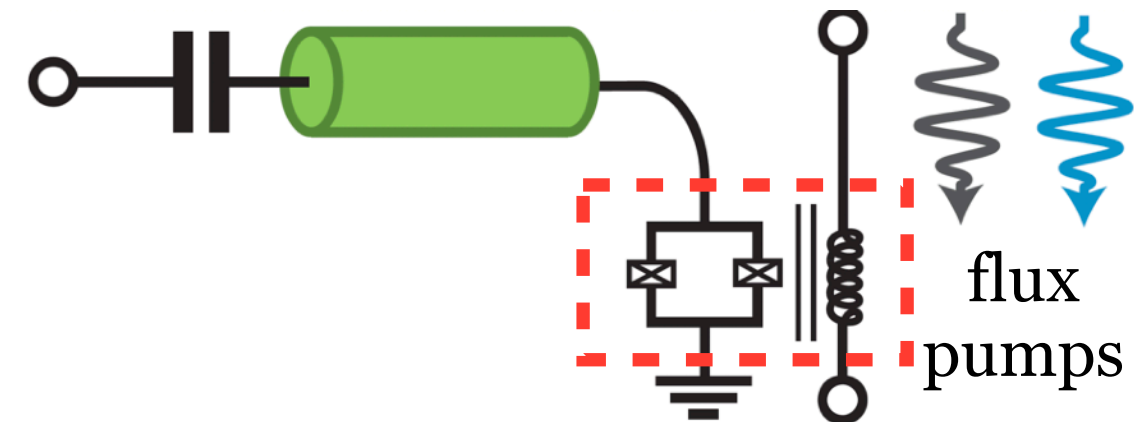


- Complex hopping terms with controllable phases
- Simulation of topological phases of matter

Fang, Yu & Fan, Nat. Photonics 6, 782 (2012)

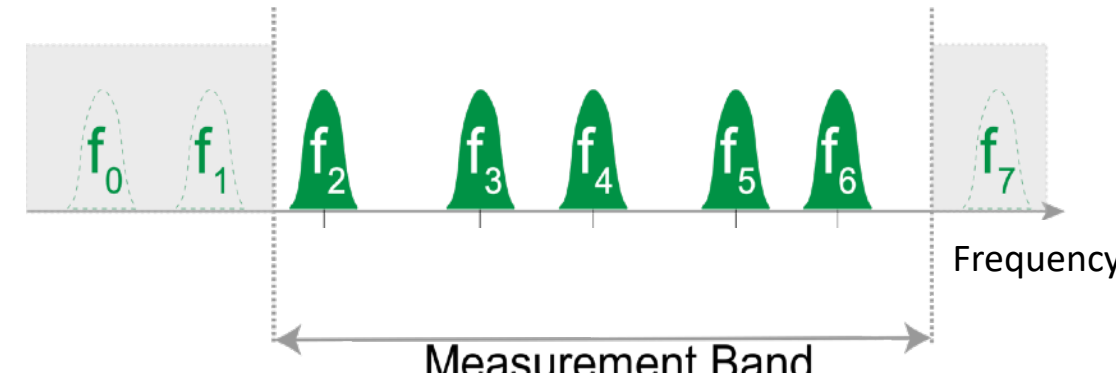
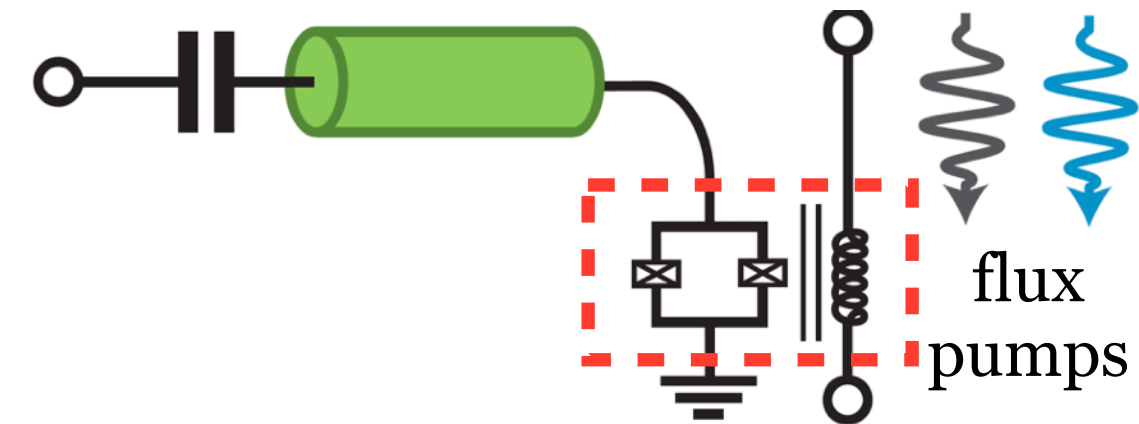
# Platform: multimode parametric cavity

- Long cavity, terminated with SQUID



# Platform: multimode parametric cavity

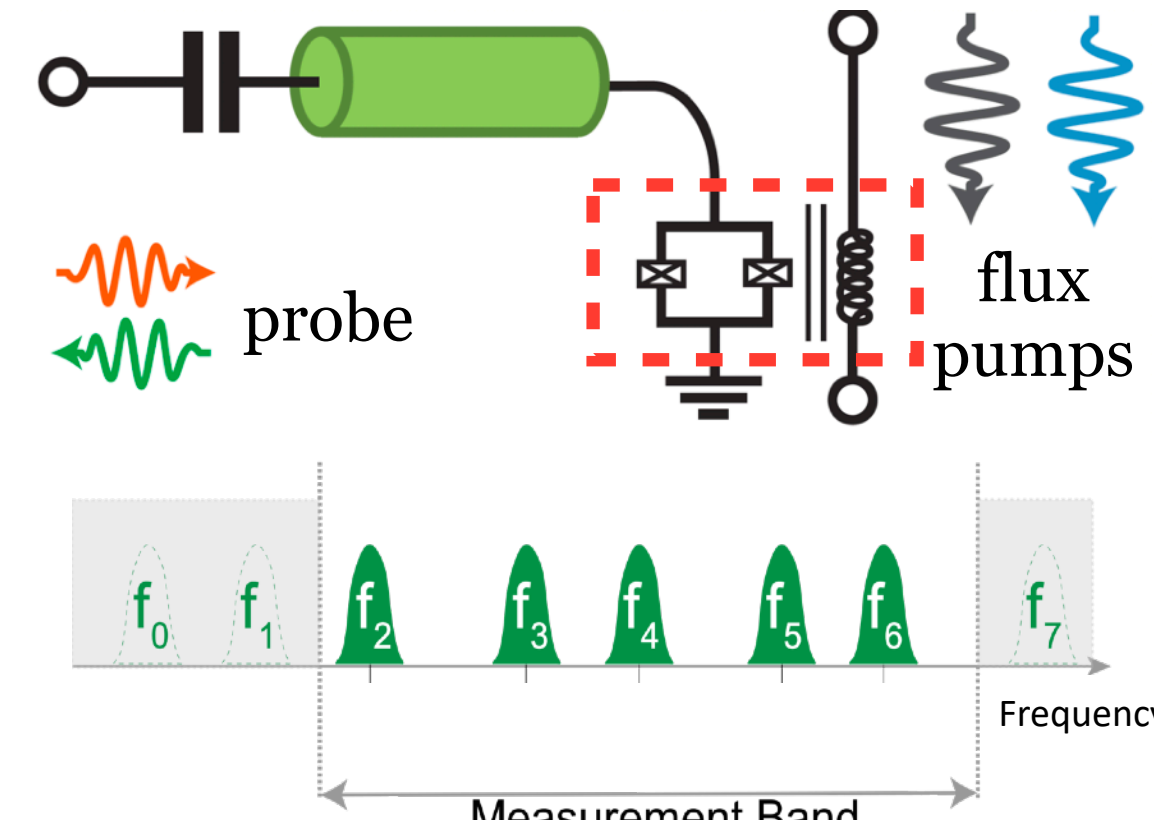
- Long cavity, terminated with SQUID
- Multiple cavity modes in measurement band
  - Lattice sites in synthetic frequency dimension!



Alaeian et al., PRA 99, 053834 (2019)  
Hung, ..., Wilson, PRL 127, 100503 (2021)

# Platform: multimode parametric cavity

- Long cavity, terminated with SQUID
- Multiple cavity modes in measurement band
  - Lattice sites in synthetic frequency dimension!
- Modes probed through scattering measurements



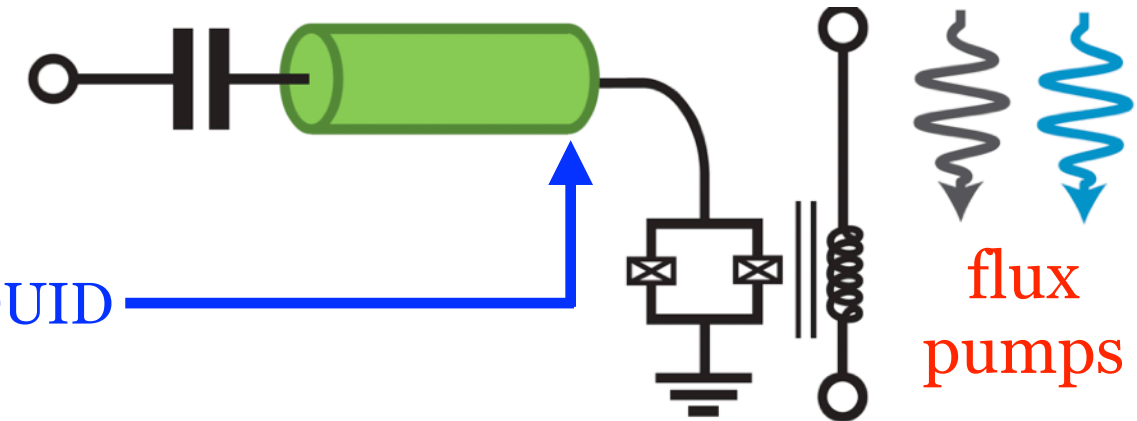
Alaeian et al., PRA 99, 053834 (2019)  
Hung, ..., Wilson, PRL 127, 100503 (2021)

# Parametric toolbox: SQUID-mediated interactions

- Symmetric SQUID:

$$\hat{H}_{\text{SQ}} = E_J \left| \cos \frac{\pi(\hat{\Phi}_p + \Phi_{\text{bias}})}{\Phi_0} \right| \cos \frac{2\pi\hat{\Phi}_{\text{cav}}}{\Phi_0}$$

Flux pump      Cavity field at SQUID



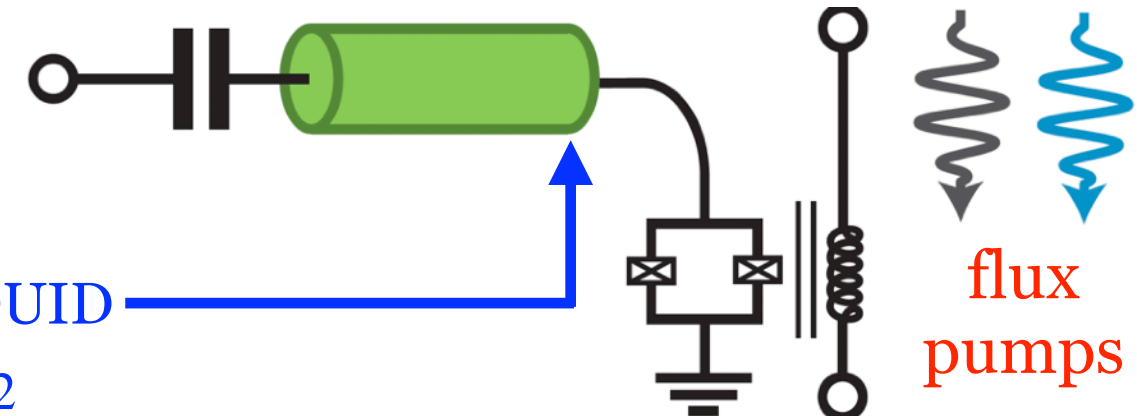
# Parametric toolbox: SQUID-mediated interactions

- Symmetric SQUID:

$$\hat{H}_{\text{SQ}} = E_J \left| \cos \frac{\pi(\hat{\Phi}_p + \Phi_{\text{bias}})}{\Phi_0} \right| \cos \frac{2\pi\hat{\Phi}_{\text{cav}}}{\Phi_0}$$

Flux pump      Cavity field at SQUID

$$\hat{H}_{\text{SQ}} \propto \hbar g_0 (\alpha_p + \alpha_p^*) (\hat{a}_1 + \hat{a}_1^\dagger + \hat{a}_2 + \hat{a}_2^\dagger + \dots)^2$$



Zakka-Bajjani et al., Nat. Phys. 7, 599 (2011)  
Flurin et al., PRL 109, 183901 (2012)  
Chang, ..., Wilson, PRAppl 10, 044019 (2018)

# Parametric toolbox: SQUID-mediated interactions

- Symmetric SQUID:

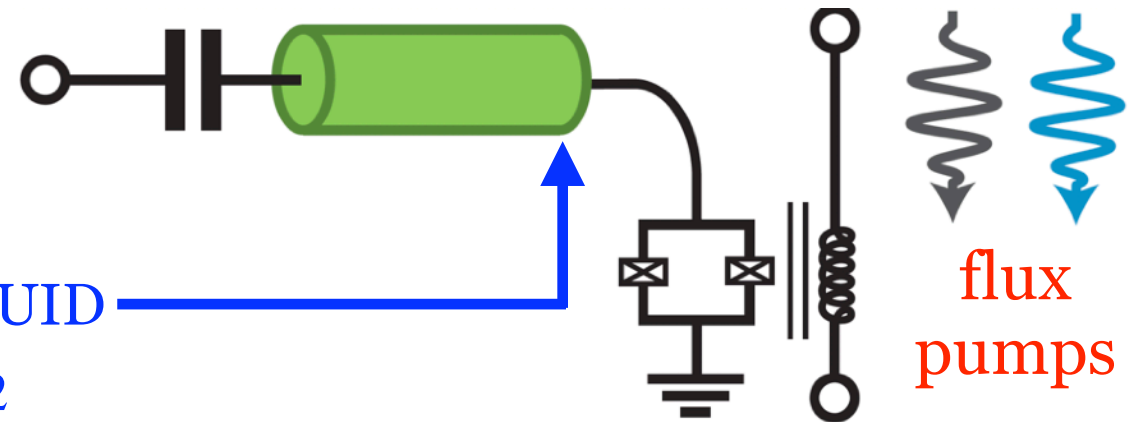
$$\hat{H}_{\text{SQ}} = E_J \left| \cos \frac{\pi(\hat{\Phi}_p + \Phi_{\text{bias}})}{\Phi_0} \right| \cos \frac{2\pi\hat{\Phi}_{\text{cav}}}{\Phi_0}$$

Flux pump      Cavity field at SQUID

$$\hat{H}_{\text{SQ}} \propto \hbar g_0 (\alpha_p + \alpha_p^*) (\hat{a}_1 + \hat{a}_1^\dagger + \hat{a}_2 + \hat{a}_2^\dagger + \dots)^2$$

- Pumping activates interactions in rotating wave approx.:

- Pump @  $f_p = |f_i - f_j|$ : hopping  $\hat{H}_{\text{BS}} \approx \hbar(g\hat{a}_i^\dagger\hat{a}_j + g^*\hat{a}_i^\dagger\hat{a}_j)$
- Pump @  $f_p = f_i + f_j$ : pairing  $\hat{H}_{\text{DC}} \approx \hbar(g\hat{a}_i\hat{a}_j + g^*\hat{a}_i^\dagger\hat{a}_j^\dagger)$



Zakka-Bajjani et al., Nat. Phys. 7, 599 (2011)  
 Flurin et al., PRL 109, 183901 (2012)  
 Chang, ..., Wilson, PRAppl 10, 044019 (2018)

# Parametric toolbox: SQUID-mediated interactions

- Symmetric SQUID:

$$\hat{H}_{\text{SQ}} = E_J \left| \cos \frac{\pi(\hat{\Phi}_p + \Phi_{\text{bias}})}{\Phi_0} \right| \cos \frac{2\pi\hat{\Phi}_{\text{cav}}}{\Phi_0}$$

Flux pump      Cavity field at SQUID

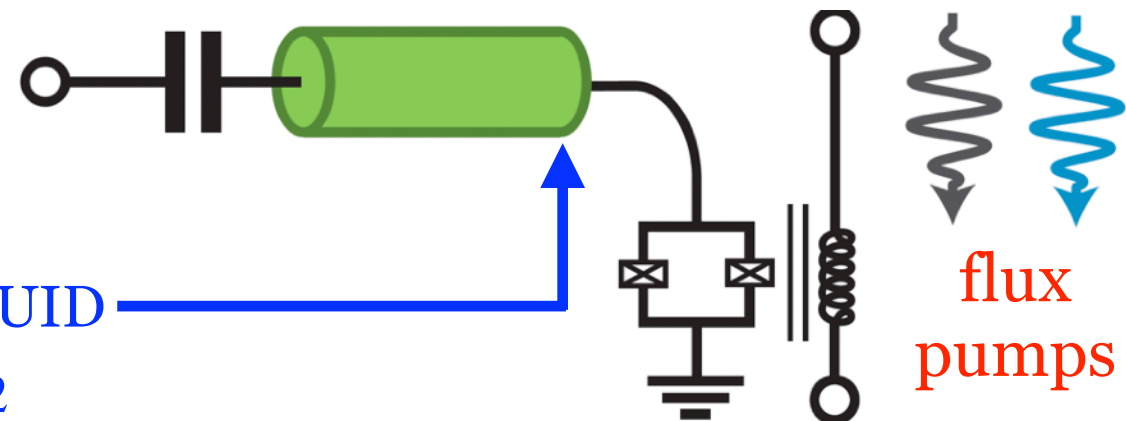
$$\hat{H}_{\text{SQ}} \propto \hbar g_0 (\alpha_p + \alpha_p^*) (\hat{a}_1 + \hat{a}_1^\dagger + \hat{a}_2 + \hat{a}_2^\dagger + \dots)^2$$

- Pumping activates interactions in rotating wave approx.:

- Pump @  $f_p = |f_i - f_j|$ : hopping  $\hat{H}_{\text{BS}} \approx \hbar(g\hat{a}_i^\dagger\hat{a}_j + g^*\hat{a}_i^\dagger\hat{a}_j)$

- Pump @  $f_p = f_i + f_j$ : pairing  $\hat{H}_{\text{DC}} \approx \hbar(g\hat{a}_i\hat{a}_j + g^*\hat{a}_i^\dagger\hat{a}_j^\dagger)$

- **In-situ tunable coupling amplitude & phase**

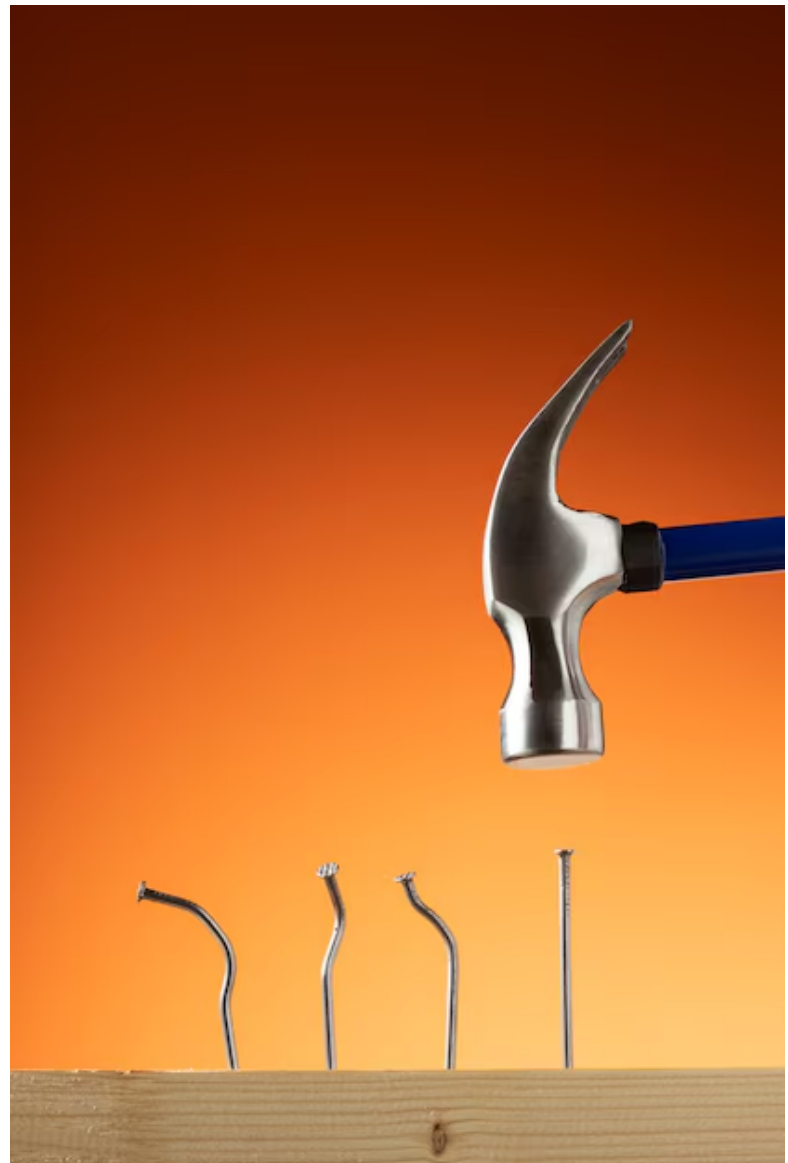


$$g = g_0 |\alpha_p| e^{i\phi}$$

Zakka-Bajjani et al., Nat. Phys. 7, 599 (2011)  
 Flurin et al., PRL 109, 183901 (2012)  
 Chang, ..., Wilson, PRAppl 10, 044019 (2018)

# Story so far

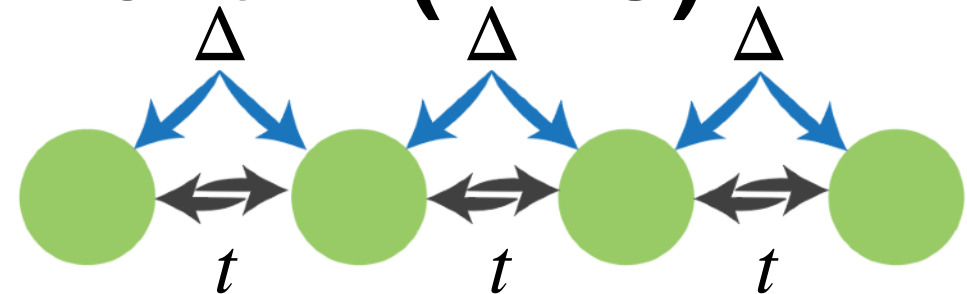
- We have bosonic lattice sites...
- ... and can customize hopping & pairing couplings between sites...
- ... so what shall we simulate?



# Target system: bosonic Kitaev chain (BKC)

$$\hat{\mathcal{H}}_B = \frac{1}{2} \sum_j (te^{i\varphi_t} \hat{a}_{j+1}^\dagger \hat{a}_j + i\Delta \hat{a}_{j+1}^\dagger \hat{a}_j^\dagger + \text{h.c.})$$

- Bosonic sites
- Hopping  $t$  and pairing  $\Delta$

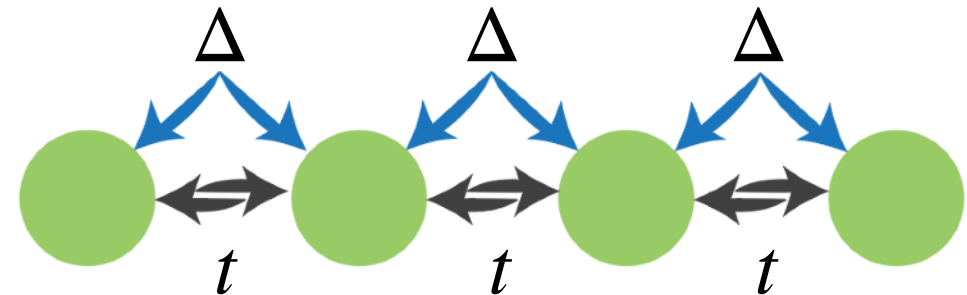


McDonald, Pereg-Barnea & Clerk, PRX 8, 041031 (2018)

# BKC: chiral transport

$$\hat{\mathcal{H}}_B = \frac{1}{2} \sum_j (te^{i\varphi_t} \hat{a}_{j+1}^\dagger \hat{a}_j + i\Delta \hat{a}_{j+1}^\dagger \hat{a}_j^\dagger + \text{h.c.})$$

- Position & momentum quadratures  $\hat{a}_j = (\hat{x}_j + i\hat{p}_j)/\sqrt{2}$



McDonald, Pereg-Barnea & Clerk, PRX 8, 041031 (2018)

# BKC: chiral transport

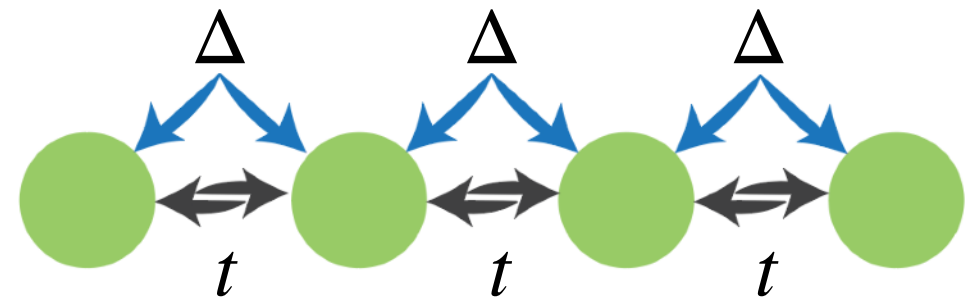
$$\hat{\mathcal{H}}_B = \frac{1}{2} \sum_j (te^{i\varphi_t} \hat{a}_{j+1}^\dagger \hat{a}_j + i\Delta \hat{a}_{j+1}^\dagger \hat{a}_j^\dagger + \text{h.c.})$$

- Position & momentum quadratures  $\hat{a}_j = (\hat{x}_j + i\hat{p}_j)/\sqrt{2}$

- Heisenberg EoM at  $\varphi_t = \pi/2$ :

$$2\hbar\dot{\hat{x}}_j = (t + \Delta)\hat{x}_{j-1} - (t - \Delta)\hat{x}_{j+1}$$

$$2\hbar\dot{\hat{p}}_j = (t - \Delta)\hat{p}_{j-1} - (t + \Delta)\hat{p}_{j+1}$$



McDonald, Pereg-Barnea & Clerk, PRX 8, 041031 (2018)

# BKC: chiral transport

$$\hat{\mathcal{H}}_B = \frac{1}{2} \sum_j (te^{i\varphi_t} \hat{a}_{j+1}^\dagger \hat{a}_j + i\Delta \hat{a}_{j+1}^\dagger \hat{a}_j^\dagger + \text{h.c.})$$

- Position & momentum quadratures  $\hat{a}_j = (\hat{x}_j + i\hat{p}_j)/\sqrt{2}$

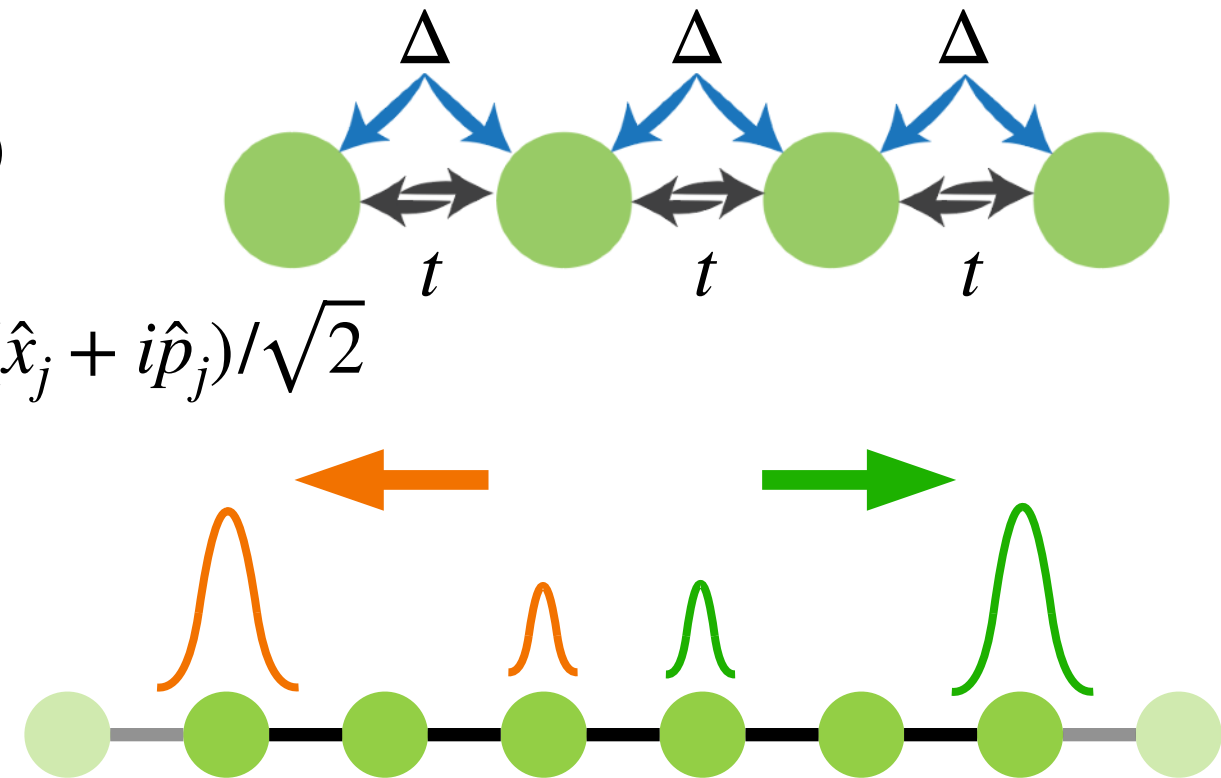
- Heisenberg EoM at  $\varphi_t = \pi/2$ :

$$2\hbar\dot{\hat{x}}_j = (t + \Delta)\hat{x}_{j-1} - (t - \Delta)\hat{x}_{j+1}$$

$$2\hbar\dot{\hat{p}}_j = (t - \Delta)\hat{p}_{j-1} - (t + \Delta)\hat{p}_{j+1}$$

- Phase-dependent chiral transport

- $\Delta \rightarrow t$  limit:  $x$  goes right,  $p$  goes left

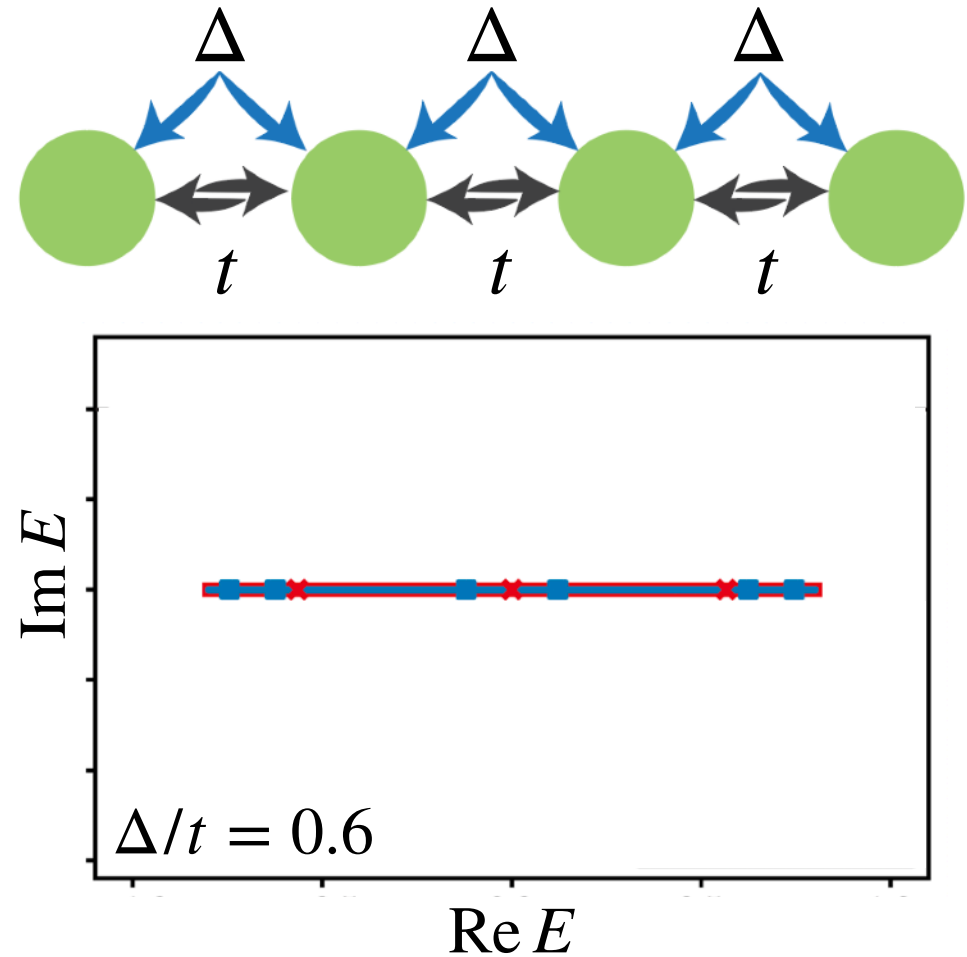


McDonald, Pereg-Barnea & Clerk, PRX 8, 041031 (2018)

# BKC: sensitivity to boundary

$$\hat{\mathcal{H}}_B = \frac{1}{2} \sum_j (te^{i\varphi_t} \hat{a}_{j+1}^\dagger \hat{a}_j + i\Delta \hat{a}_{j+1}^\dagger \hat{a}_j^\dagger + \text{h.c.})$$

- Open boundary spectrum: always real
- Periodic boundary spectrum:
  - $t |\cos \varphi_t| > \Delta$ : real

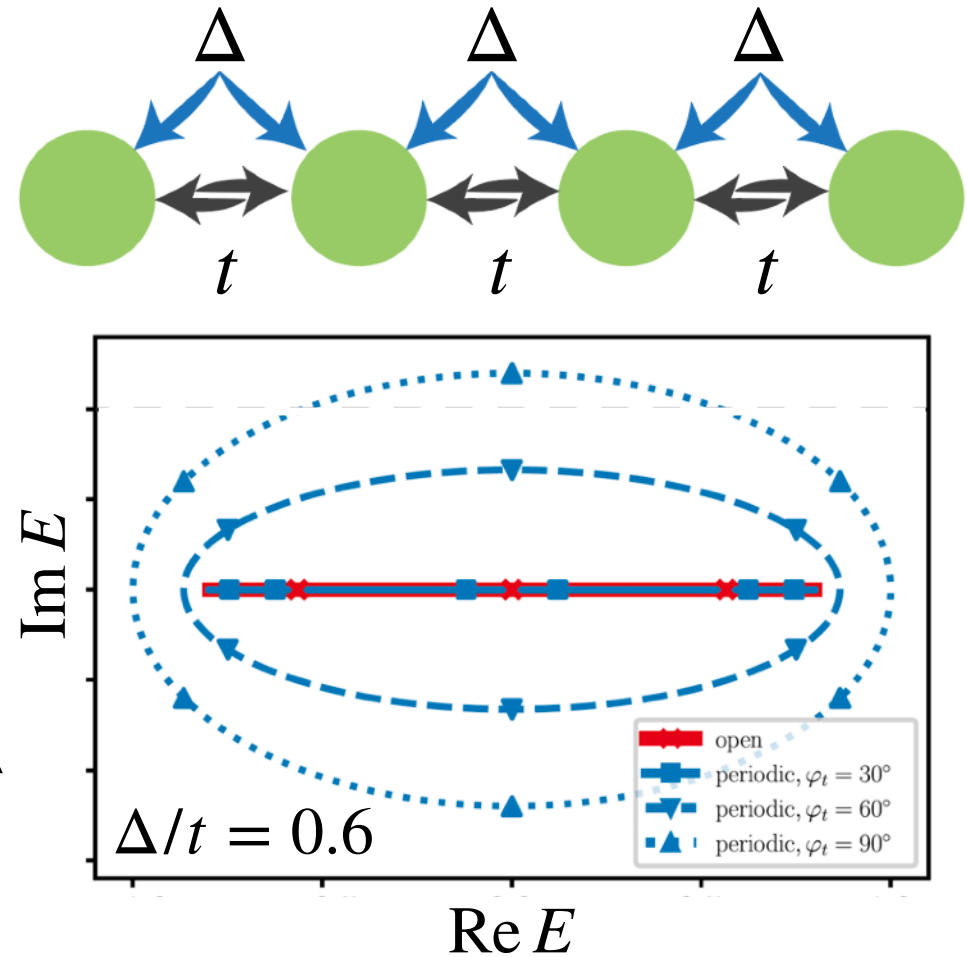


Okuma et al., PRL 124, 086801 (2020)  
Busnaina, ..., Wilson, Nat. Commun. 15, 3065 (2024)

# BKC: sensitivity to boundary

$$\hat{\mathcal{H}}_B = \frac{1}{2} \sum_j (te^{i\varphi_t} \hat{a}_{j+1}^\dagger \hat{a}_j + i\Delta \hat{a}_{j+1}^\dagger \hat{a}_j^\dagger + \text{h.c.})$$

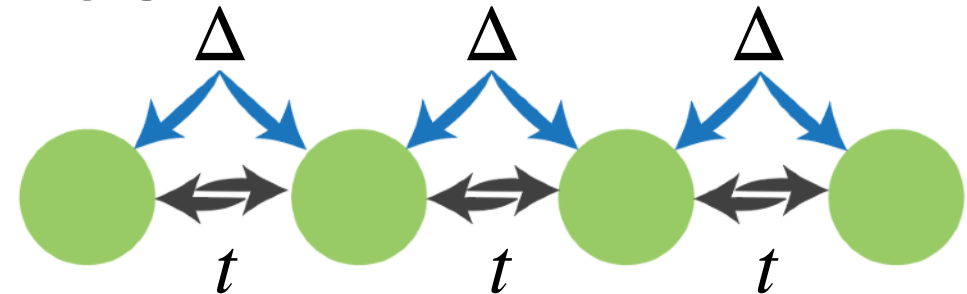
- Open boundary spectrum: always real
- Periodic boundary spectrum:
  - $t |\cos \varphi_t| > \Delta$ : real
  - $t |\cos \varphi_t| < \Delta$ : complex (nontrivial winding)
  - Topological phase transition @  $t |\cos \varphi_t| = \Delta$



Okuma et al., PRL 124, 086801 (2020)  
Busnaina, ..., Wilson, Nat. Commun. 15, 3065 (2024)

# BKC: “non-Hermitian” skin effect

$$\hat{\mathcal{H}}_B = \frac{1}{2} \sum_j (te^{i\varphi_t} \hat{a}_{j+1}^\dagger \hat{a}_j + i\Delta \hat{a}_{j+1}^\dagger \hat{a}_j^\dagger + \text{h.c.})$$

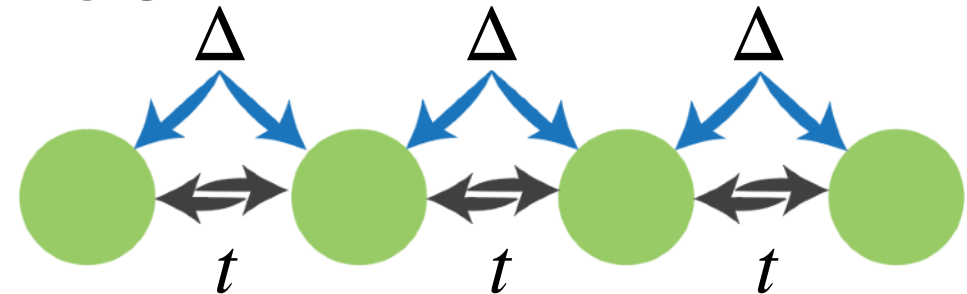


Switching back to open boundary:

- $t |\cos \varphi_t| > \Delta$ : eigenstates are plane waves
- $t |\cos \varphi_t| < \Delta$ : eigenstates **concentrated at edges**

# BKC: “non-Hermitian” skin effect

$$\hat{\mathcal{H}}_B = \frac{1}{2} \sum_j (te^{i\varphi_t} \hat{a}_{j+1}^\dagger \hat{a}_j + i\Delta \hat{a}_{j+1}^\dagger \hat{a}_j^\dagger + \text{h.c.})$$



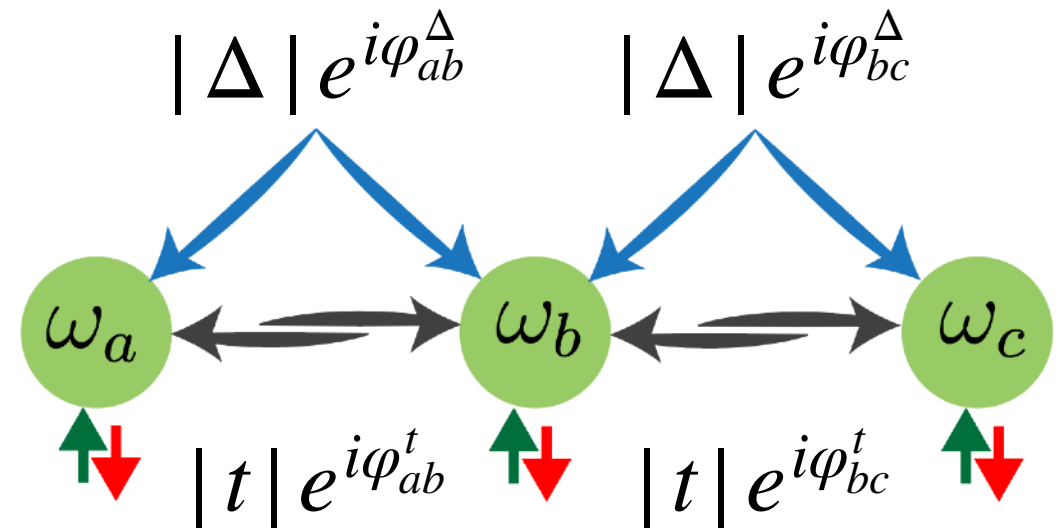
Switching back to open boundary:

- $t |\cos \varphi_t| > \Delta$ : eigenstates are plane waves
- $t |\cos \varphi_t| < \Delta$ : eigenstates **concentrated at edges**
- “Non-Hermitian” skin effect – topological origin
  - Heisenberg EoM **effectively** non-Hermitian (bosons!)

Okuma et al., PRL 124, 086801 (2020)  
Busnaina, ..., Wilson, Nat. Commun. 15, 3065 (2024)

# Simulating an open chain: link phases

- 3 sites...
- Already many phase degrees of freedom
- Sum & difference phases for each link:  
 $\varphi^\pm = (\varphi^t \pm \varphi^\Delta)/2$



Busnaina, ..., Wilson, Nat. Commun. 15, 3065 (2024)

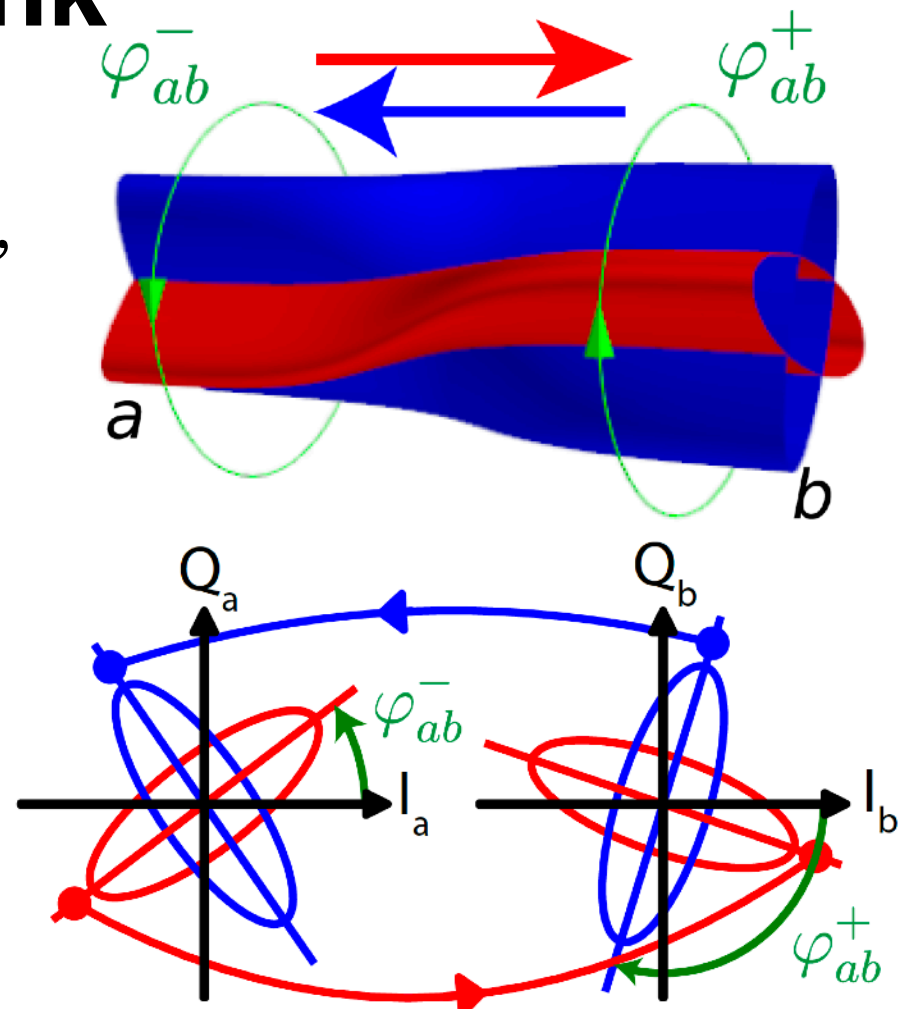
# Twisted-tubes picture: single link

- Phase-dependent chiral transport
  - In a given direction, some quadratures amplified, others attenuated

Busnaina, ..., Wilson, Nat. Commun. 15, 3065 (2024)

# Twisted-tubes picture: single link

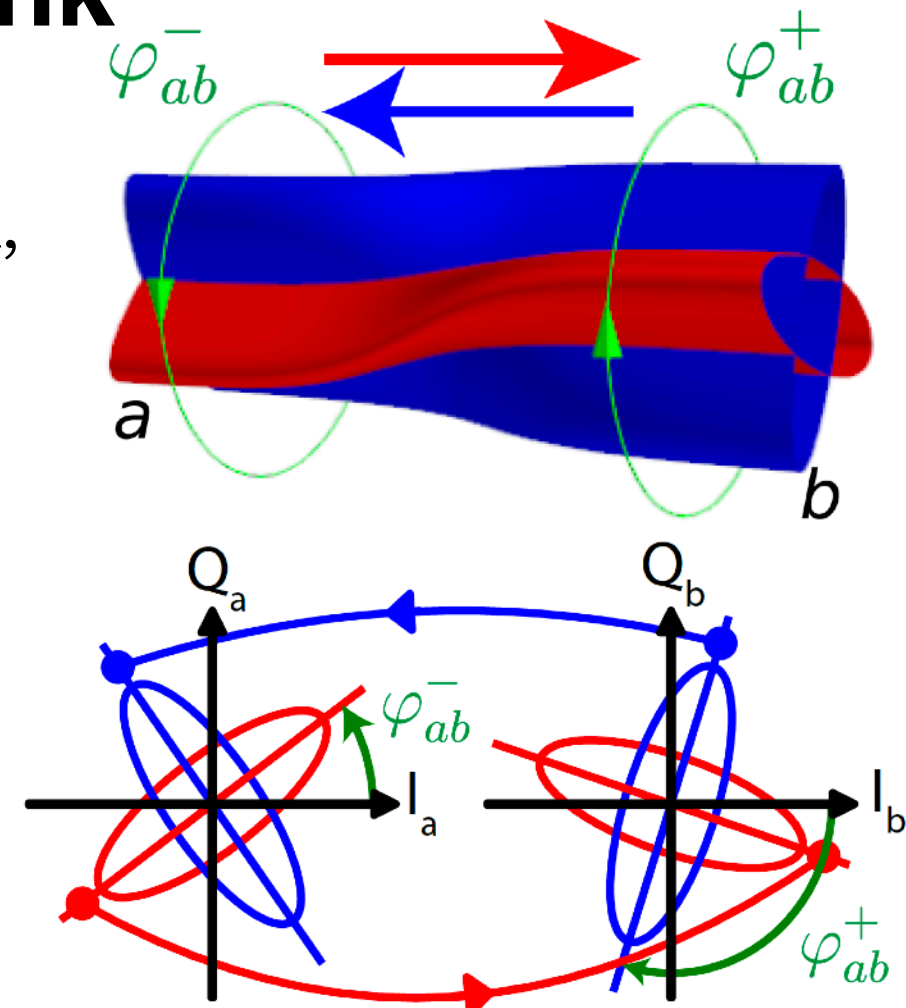
- Phase-dependent chiral transport
  - In a given direction, some quadratures amplified, others attenuated
- $a$ - $b$  tubes
  - Amplified from  $a$  to  $b$ : major axis of red ellipse
  - Amplified from  $b$  to  $a$ : major axis of blue ellipse



Busnaina, ..., Wilson, Nat. Commun. 15, 3065 (2024)

# Twisted-tubes picture: single link

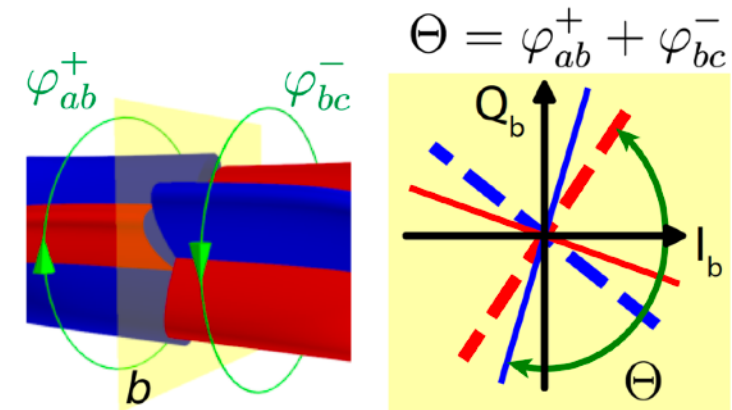
- Phase-dependent chiral transport
  - In a given direction, some quadratures amplified, others attenuated
- $a$ - $b$  tubes
  - Amplified from  $a$  to  $b$ : major axis of red ellipse
  - Amplified from  $b$  to  $a$ : major axis of blue ellipse
  - Changing  $\varphi_{ab}^-$  twists the tubes at  $a$
  - Changing  $\varphi_{ab}^+$  twists the tubes at  $b$ 
    - These are just “gauge transformations”!
    - Can compensate by locally redefining quadratures



# Twisted-tubes picture: more links

- We **cannot** “gauge away” the relative misalignment between two tubes  $a-b$  and  $b-c$ !
- Gauge-invariant phase  $\Theta = \varphi_{ab}^+ + \varphi_{bc}^-$

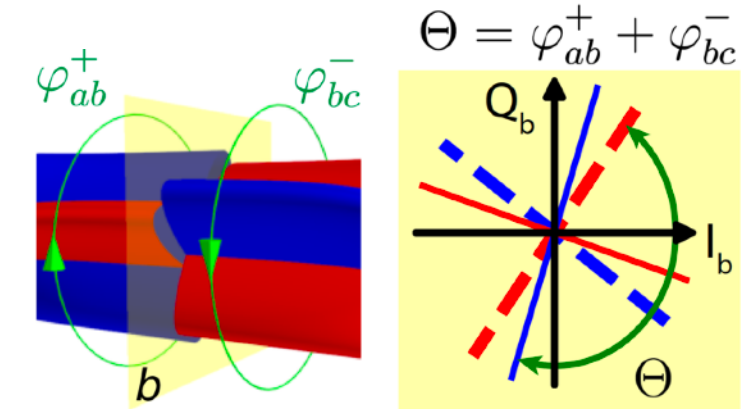
Arbitrary misalignment



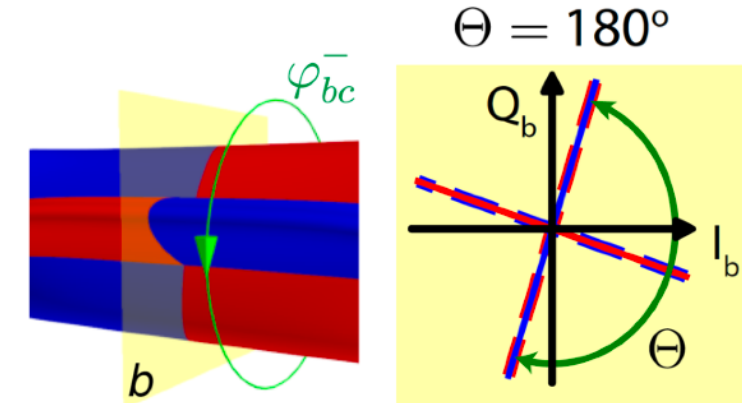
# Twisted-tubes picture: more links

- We **cannot** “gauge away” the relative misalignment between two tubes  $a-b$  and  $b-c$ !
- Gauge-invariant phase  $\Theta = \varphi_{ab}^+ + \varphi_{bc}^-$
- Maximal misalignment:  $\Theta = \pi$ , “trivial” chain
  - Injecting in  $b$ , transport to equally  $a$  &  $c$

Arbitrary misalignment



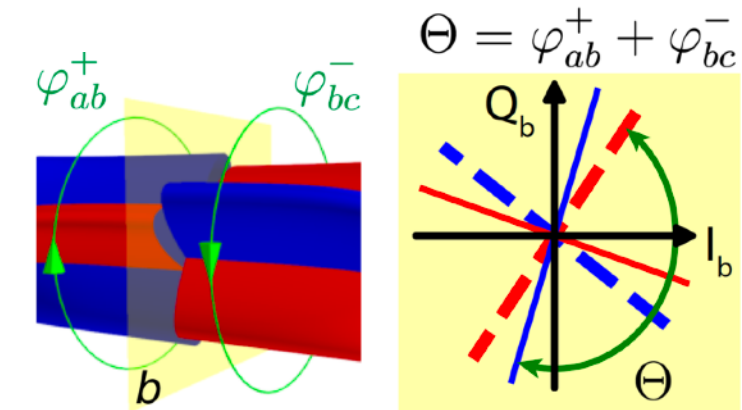
Maximal misalignment – “trivial” chain



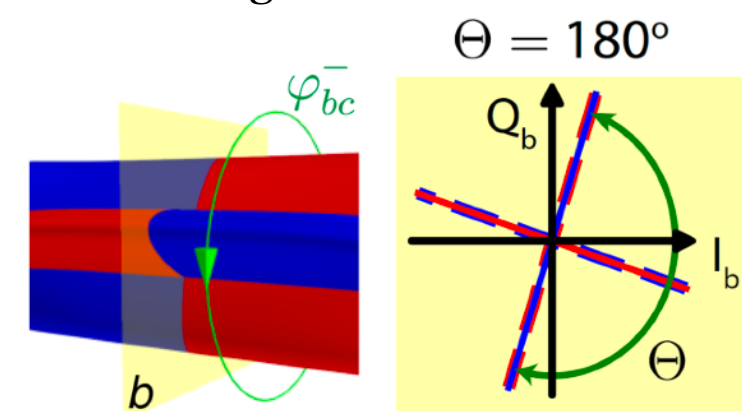
# Twisted-tubes picture: more links

- We **cannot** “gauge away” the relative misalignment between two tubes  $a-b$  and  $b-c$ !
- **Gauge-invariant phase**  $\Theta = \varphi_{ab}^+ + \varphi_{bc}^-$
- Maximal misalignment:  $\Theta = \pi$ , “trivial” chain
  - Injecting in  $b$ , transport to equally  $a$  &  $c$
- Maximal alignment:  $\Theta = \pi/2$ , “chiral” chain
  - Injecting in  $b$ , transport to mostly either  $a$  or  $c$ , depending on phase

Arbitrary misalignment



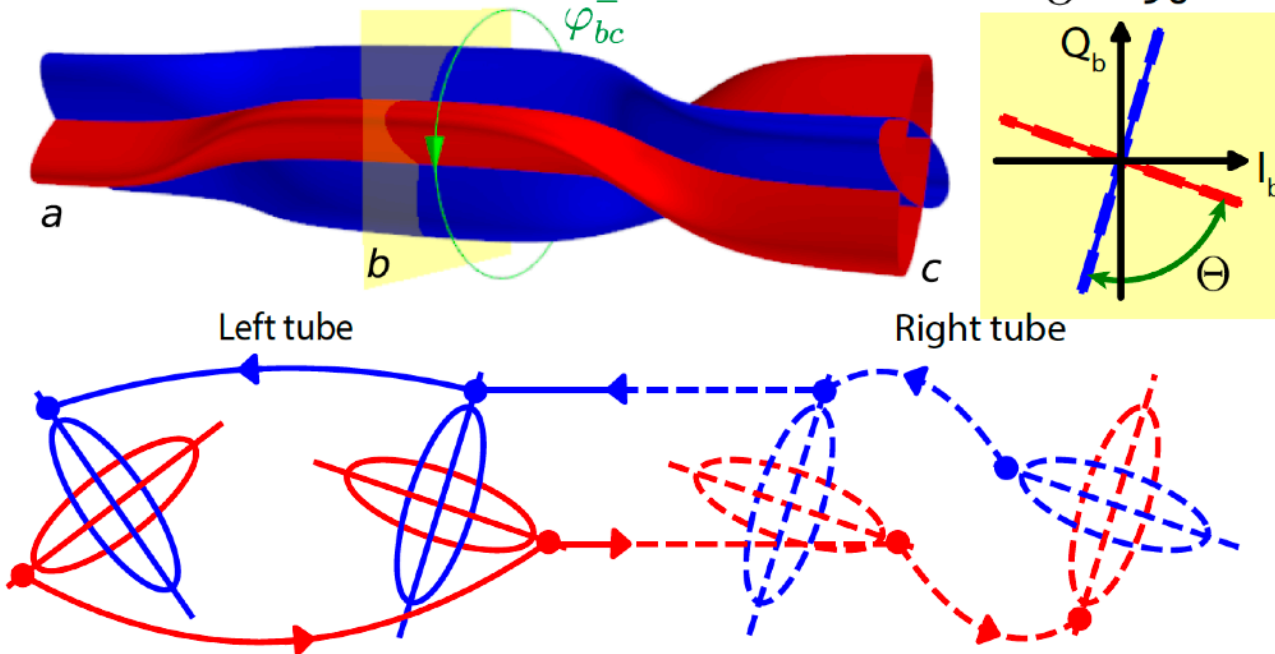
Maximal misalignment – “trivial” chain



# Twisted-tubes picture: more links

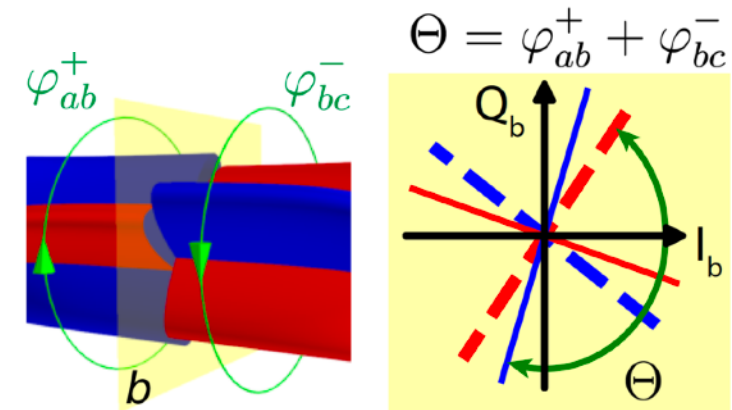
- We **cannot** “gauge away” the relative misalignment between two tubes  $a-b$  and  $b-c$ !
- Gauge-invariant phase  $\Theta = \varphi_{ab}^+ + \varphi_{bc}^-$

Maximal alignment – “chiral” chain

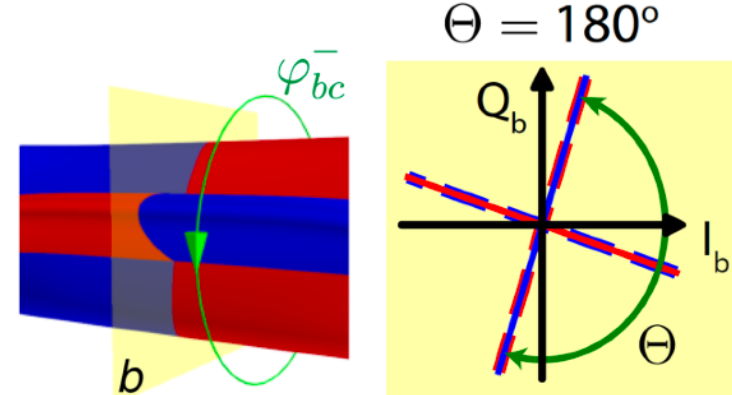


32

Arbitrary misalignment

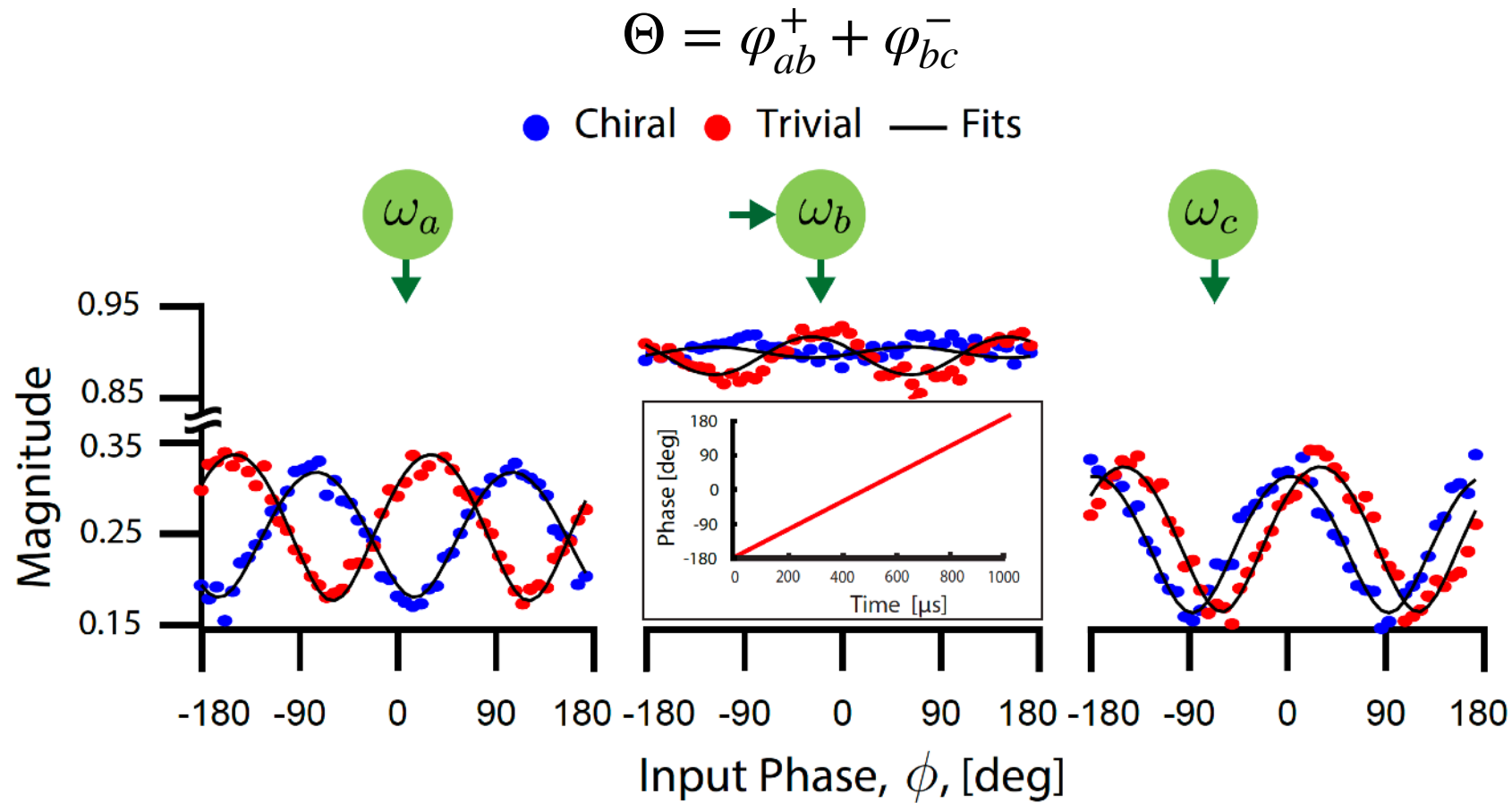


Maximal misalignment – “trivial” chain



# Open chain: calibrating tube alignment

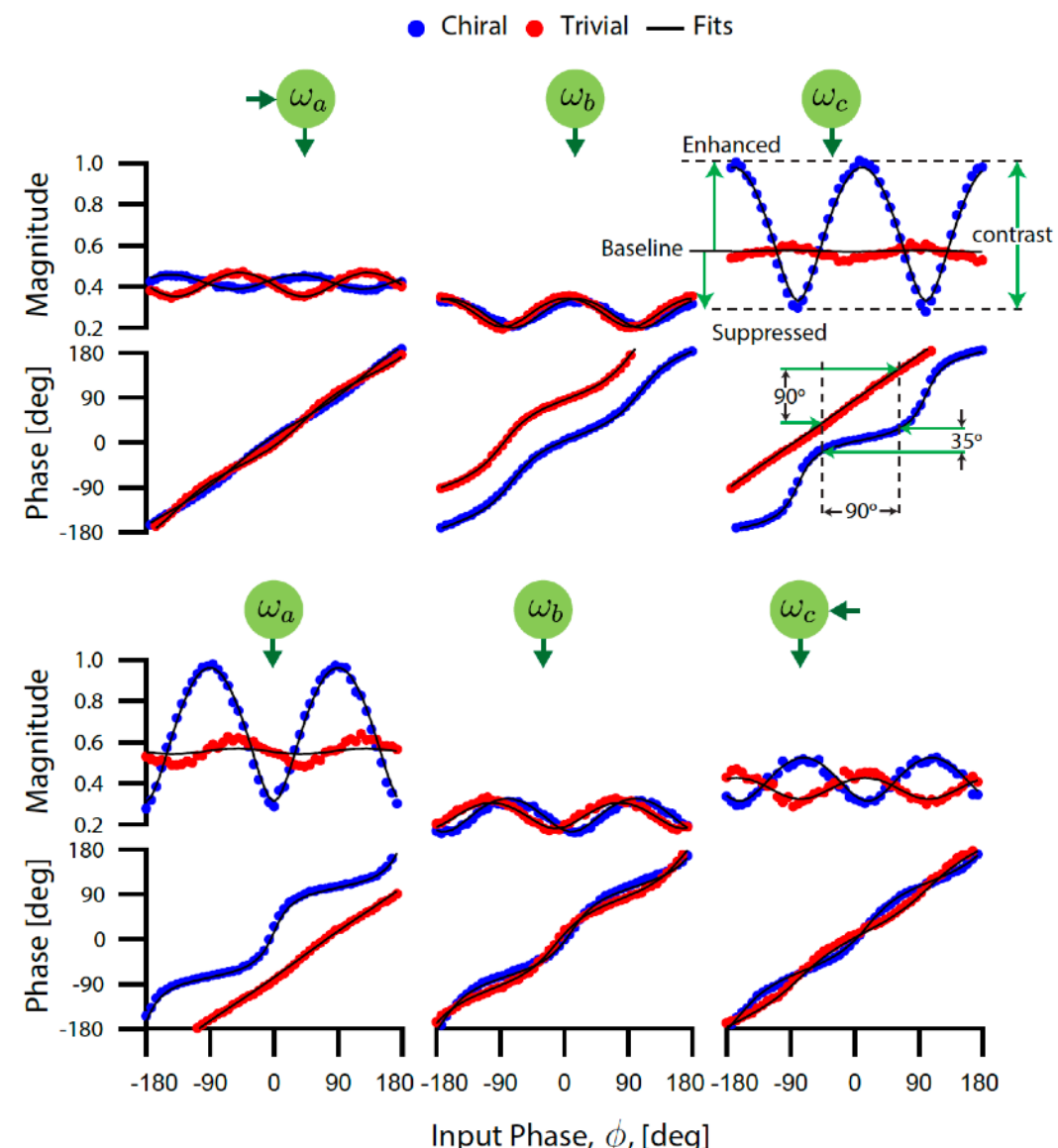
- Injecting in  $b$
- Sweeping input phase
- Sweeping  $\varphi_{ab}^+$ 
  - Transport to  $a$  changes
  - Transport to  $c$  mostly the same



Busnaina, ..., Wilson, Nat. Commun. 15, 3065 (2024)

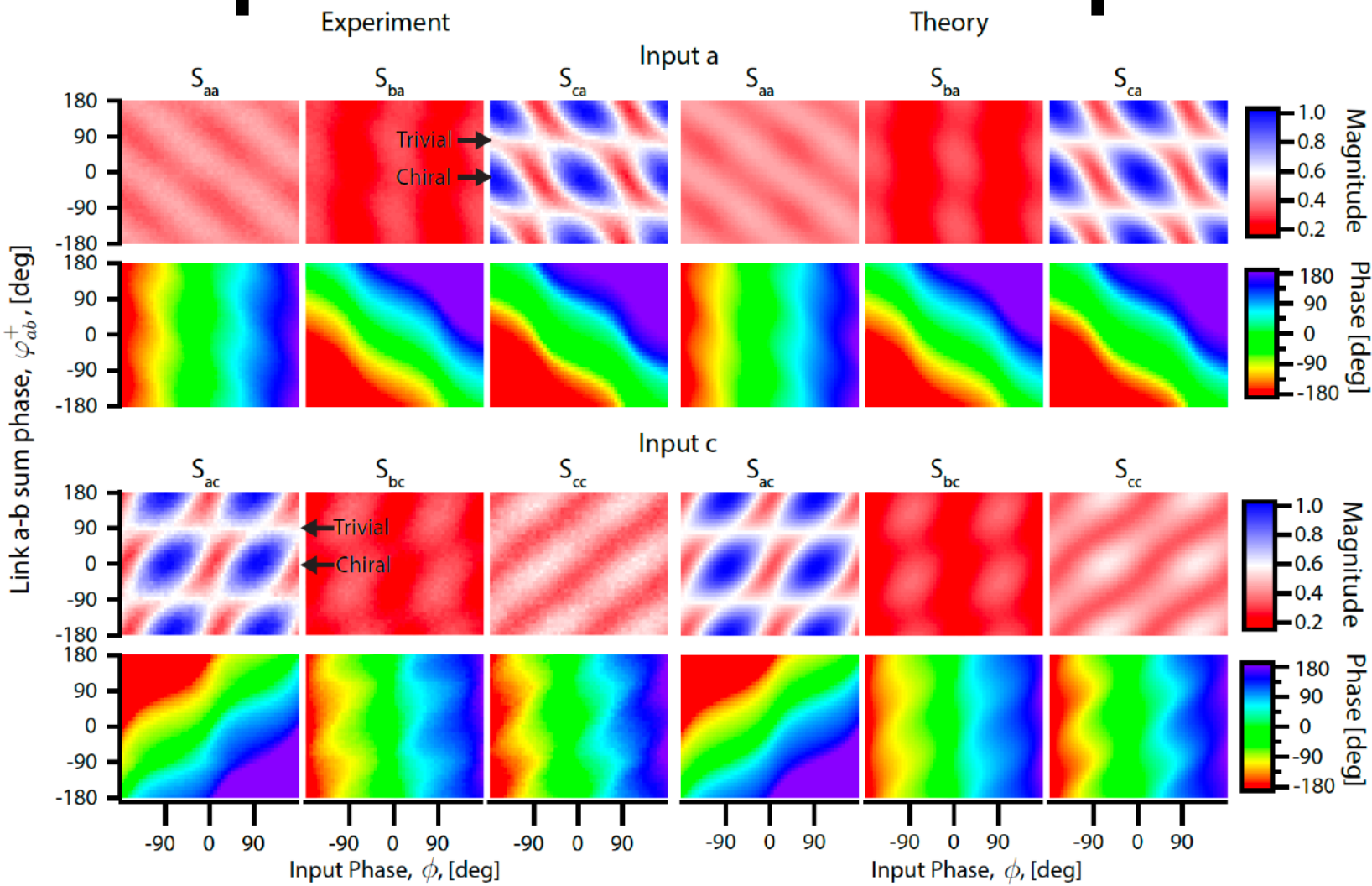
# Open chain: phase-dependent chiral transport

- Injecting in  $a$  or  $c$
- Sweeping input phase
- Regime of **chiral transport**:
  - Greater contrast in magnitude
  - Phase flattening



# Open chain: phase-dependent chiral transport

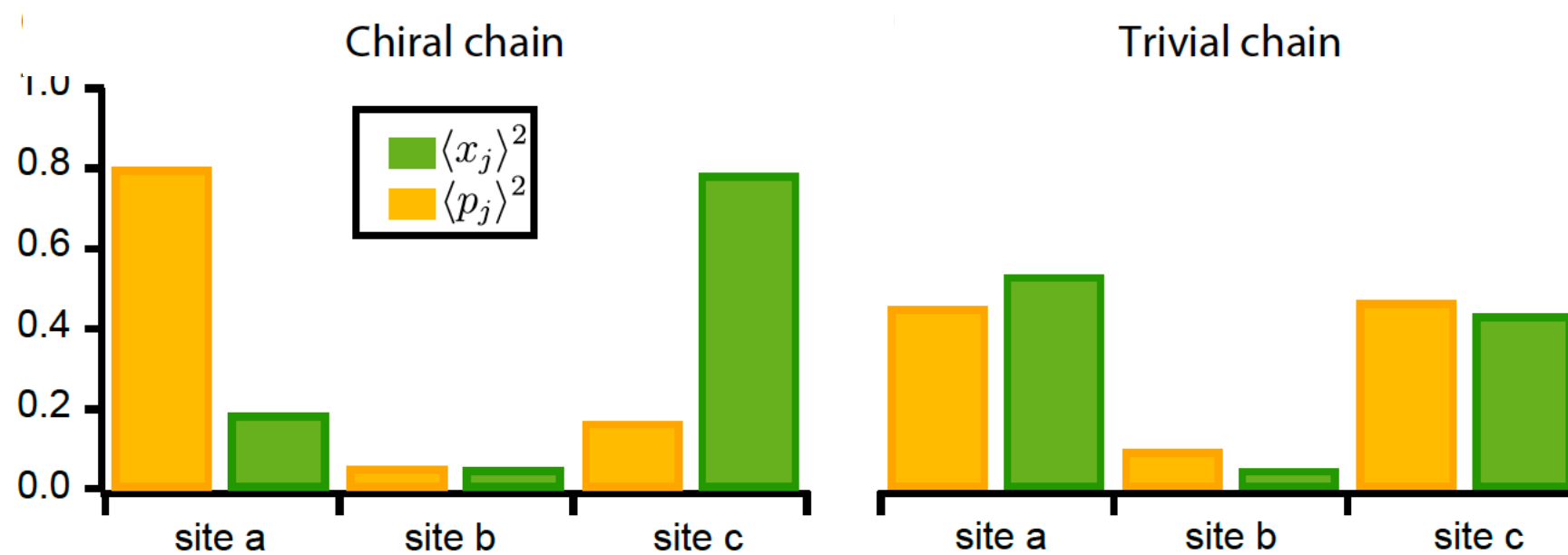
- Injecting in  $a$  or  $c$
- Sweeping input phase
- Sweeping  $\varphi_{ab}^+$



# Open chain: “non-Hermitian” skin effect

Wave functions

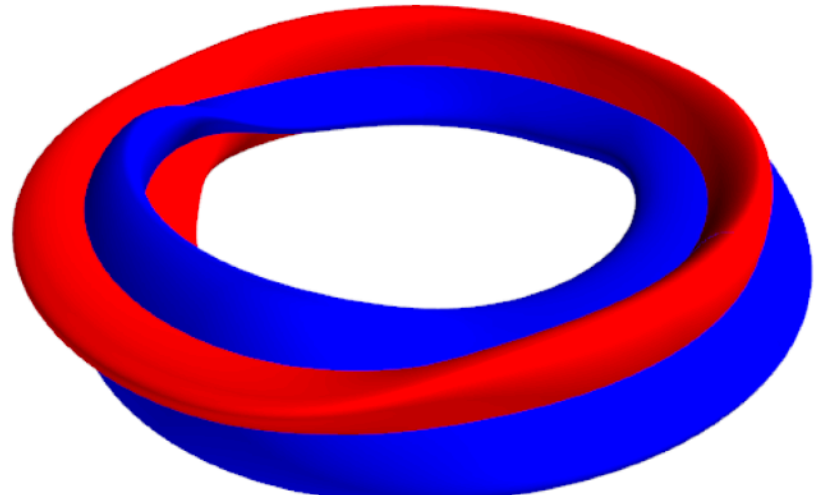
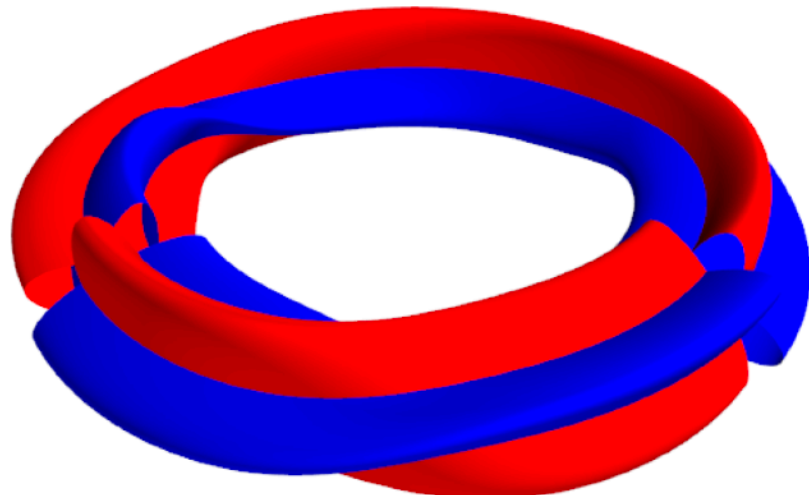
- Trivial chain: plane waves
- Chiral chain: orthogonal quadratures localized at opposite edges



Busnaina, ..., Wilson, Nat. Commun. 15, 3065 (2024)

# Closed chain: tubes

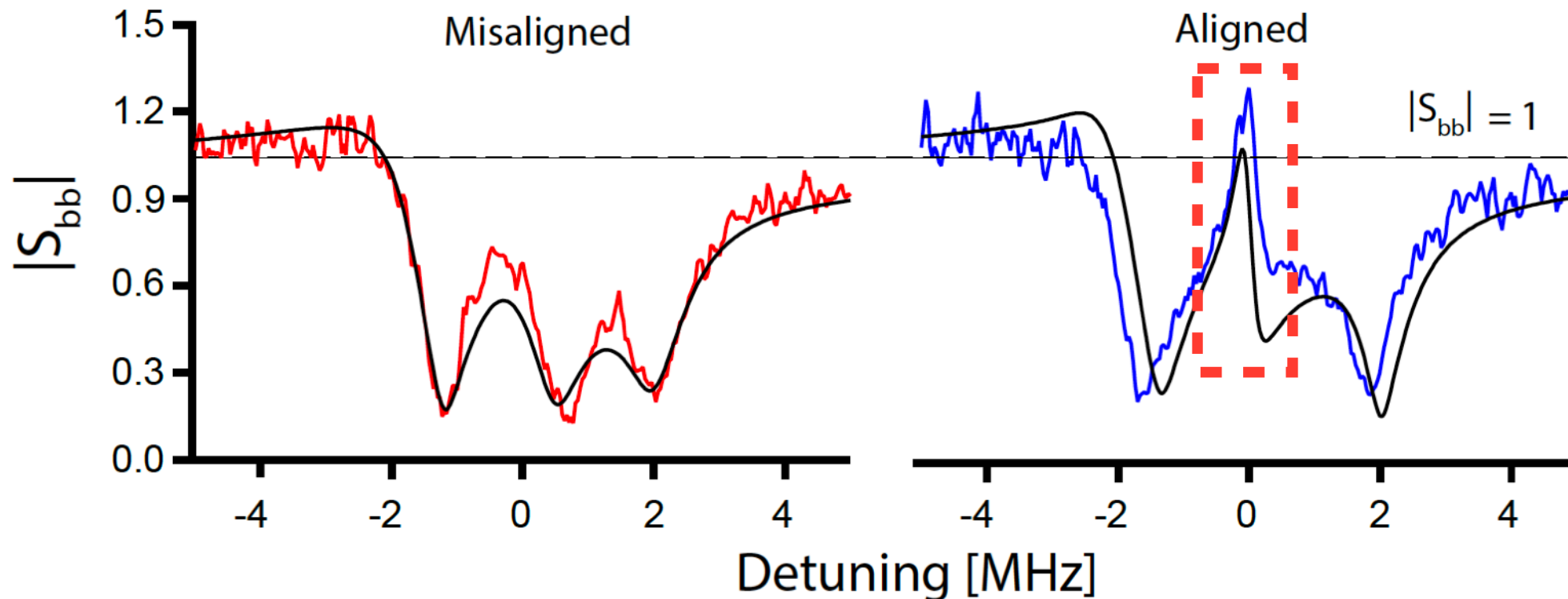
- 3 sites again
- Chiral chain: approaching **dynamical instability!**



Busnaina, ..., Wilson, Nat. Commun. 15, 3065 (2024)

# Closed chain: sensitivity to boundary

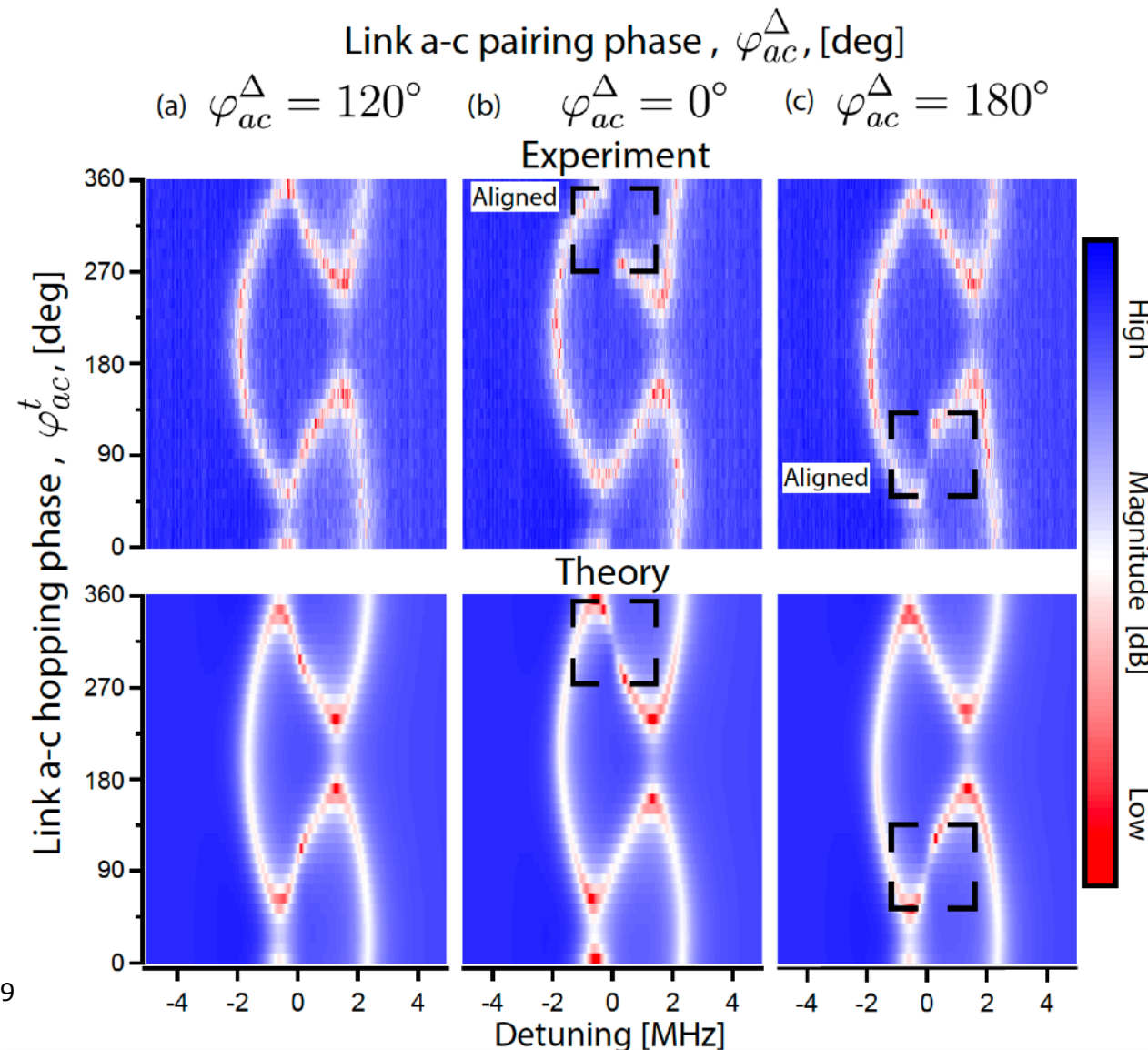
- Chiral chain: approaching **dynamical instability**
- **Peak in reflection amplitude** – finite height due to dissipation



Busnaina, ..., Wilson, Nat. Commun. 15, 3065 (2024)

# Closed chain: sensitivity to boundary

- Chiral chain: approaching **dynamical instability**
- **Peak in reflection amplitude** – finite height due to dissipation



# Conclusion I: bosonic Kitaev chain

- Bosonic lattice model with hopping & pairing
- Simulation using multimode parametric cavity

Busnaina, ZS, McDonald, Dubyna, Nsanzineza, Hung, Chang, Clerk & Wilson,  
Nat. Commun. 15, 3065 (2024)

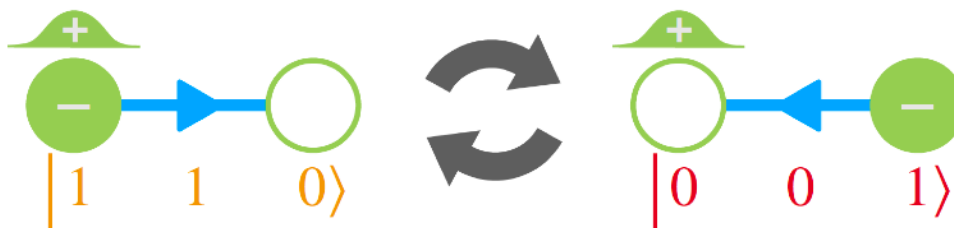
# Conclusion I: bosonic Kitaev chain

- Bosonic lattice model with hopping & pairing
- Simulation using multimode parametric cavity
- **Effective non-Hermitian** dynamics via coherent pairing
  - Phase-dependent chiral transport
  - Non-Hermitian skin effect
- Outlook: simulating genuinely quantum (i.e. coherent) non-Hermitian dynamics

Busnaina, ZS, McDonald, Dubyna, Nsanzineza, Hung, Chang, Clerk & Wilson,  
Nat. Commun. 15, 3065 (2024)

# ANALOG QUANTUM SIMULATION OF LATTICE GAUGE THEORIES

Busnaina, ZS, Alcaine-Cuervo, Yang, Nsanzineza, Rico & Wilson  
in preparation



# Background: lattice gauge theories

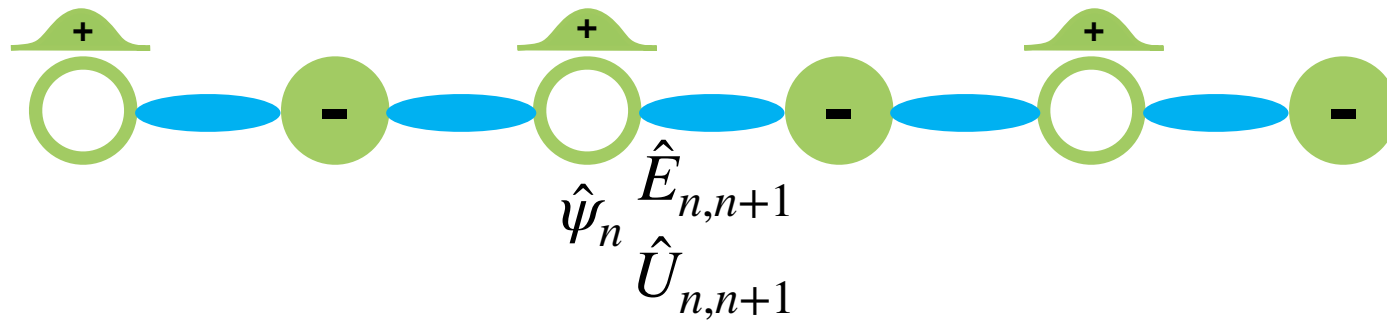
- Gauge theories
  - High-energy, condensed matter, quantum information
- Lattice gauge theories (LGT)
  - Powerful numerical techniques on classical computers
  - Difficulties remain: topological terms, finite density, growing entanglement in time evolution...
- Quantum simulation

Bañuls et al., Eur. Phys. J. D 74, 165 (2020)

# A simple case: (1+1)D quantum electrodynamics

$$\hat{\mathcal{H}} = -J \sum_{n=1}^{L-1} (\hat{\psi}_n^\dagger \hat{U}_{n,n+1} \hat{\psi}_{n+1} + \text{h.c.}) + \mu \sum_{n=1}^L (-1)^n \hat{\psi}_n^\dagger \hat{\psi}_n + V \sum_{n=1}^{L-1} \hat{E}_{n,n+1}^2$$

Matter-gauge coupling      Fermion mass      Electric field energy



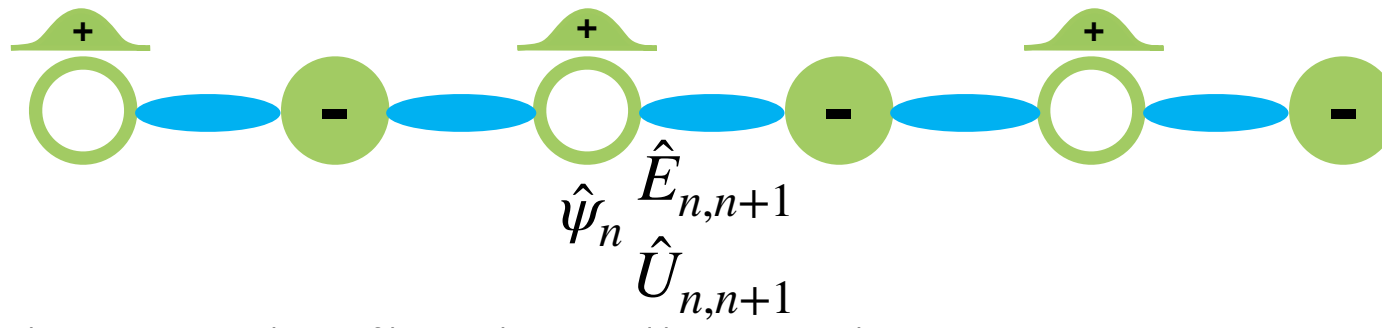
Analog quantum simulation of bosonic lattices and lattice gauge theories

# A simple case: (1+1)D quantum electrodynamics

$$\hat{\mathcal{H}} = -J \sum_{n=1}^{L-1} (\hat{\psi}_n^\dagger \hat{U}_{n,n+1} \hat{\psi}_{n+1} + \text{h.c.}) + \mu \sum_{n=1}^L (-1)^n \hat{\psi}_n^\dagger \hat{\psi}_n + V \sum_{n=1}^{L-1} \hat{E}_{n,n+1}^2$$

Matter-gauge coupling      Fermion mass      Electric field energy

- Staggered fermions  $\hat{\psi}_n$ : mobile neg. charge on static pos. background
- $U(1)$  gauge field on links  $[\hat{E}_{n,n+1}, \hat{U}_{n,n+1}] = \hat{U}_{n,n+1}$



Analog quantum simulation of bosonic lattices and lattice gauge theories

45

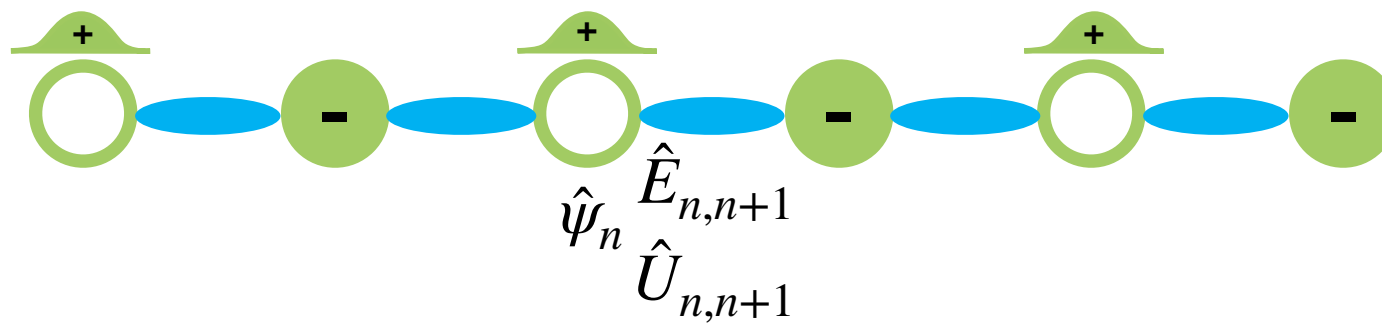
Yang et al., PRA 94, 052321 (2016)

# A simple case: (1+1)D quantum electrodynamics

$$\hat{\mathcal{H}} = -J \sum_{n=1}^{L-1} (\hat{\psi}_n^\dagger \hat{U}_{n,n+1} \hat{\psi}_{n+1} + \text{h.c.}) + \mu \sum_{n=1}^L (-1)^n \hat{\psi}_n^\dagger \hat{\psi}_n + V \sum_{n=1}^{L-1} \hat{E}_{n,n+1}^2$$

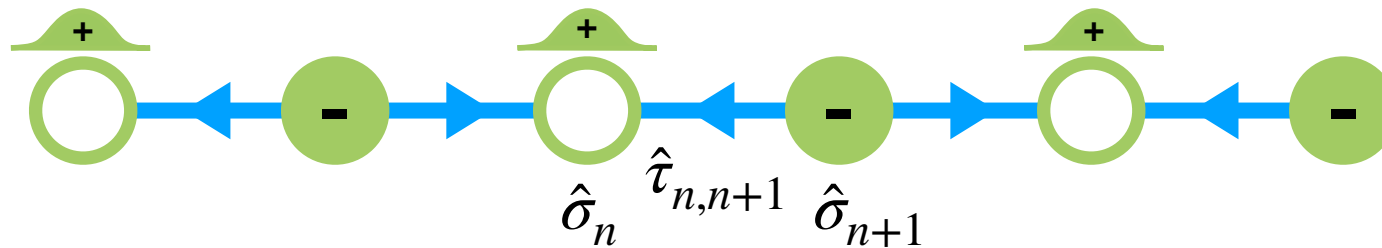
Matter-gauge coupling      Fermion mass      Electric field energy

- Staggered fermions  $\hat{\psi}_n$ : mobile neg. charge on static pos. background
- $U(1)$  gauge field on links  $[\hat{E}_{n,n+1}, \hat{U}_{n,n+1}] = \hat{U}_{n,n+1}$
- **Gauss's law**  $\hat{G}_n = \hat{\psi}_n^\dagger \hat{\psi}_n + \frac{1}{2}[(-1)^n - 1] - (\hat{E}_{n,n+1} - \hat{E}_{n-1,n})$ ;  $\hat{G}_n |\psi_{\text{phys}}\rangle = 0$



# From (1+1)D QED to U(1) spin-1/2

- Map fermions to spin-1/2 (Jordan-Wigner)
- Truncate gauge field to spin-1/2:  $\hat{E}_{n,n+1} \rightarrow \hat{\tau}_{n,n+1}^z/2$ ,  $\hat{U}_{n,n+1} \rightarrow \hat{\tau}_{n,n+1}^+$



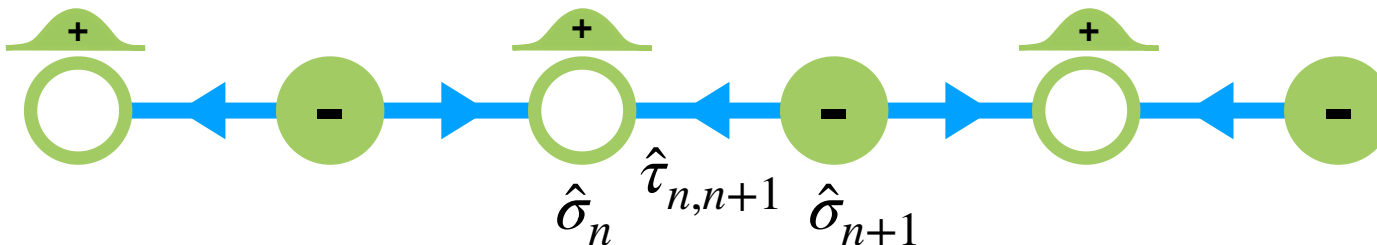
Banerjee et al., PRL 109, 175302 (2012)  
Yang et al., PRA 94, 052321 (2016)

# From (1+1)D QED to U(1) spin-1/2

- Map fermions to spin-1/2 (Jordan-Wigner)
- Truncate gauge field to spin-1/2:  $\hat{E}_{n,n+1} \rightarrow \hat{\tau}_{n,n+1}^z/2$ ,  $\hat{U}_{n,n+1} \rightarrow \hat{\tau}_{n,n+1}^+$

$$\hat{\mathcal{H}} = -J \sum_{n=1}^{L-1} (\hat{\sigma}_n^+ \hat{\tau}_{n,n+1}^+ \hat{\sigma}_{n+1}^- + \text{h.c.}) + \frac{\mu}{2} \sum_{n=1}^L (-1)^n \hat{\sigma}_n^z$$

- Transverse three-qubit interaction!



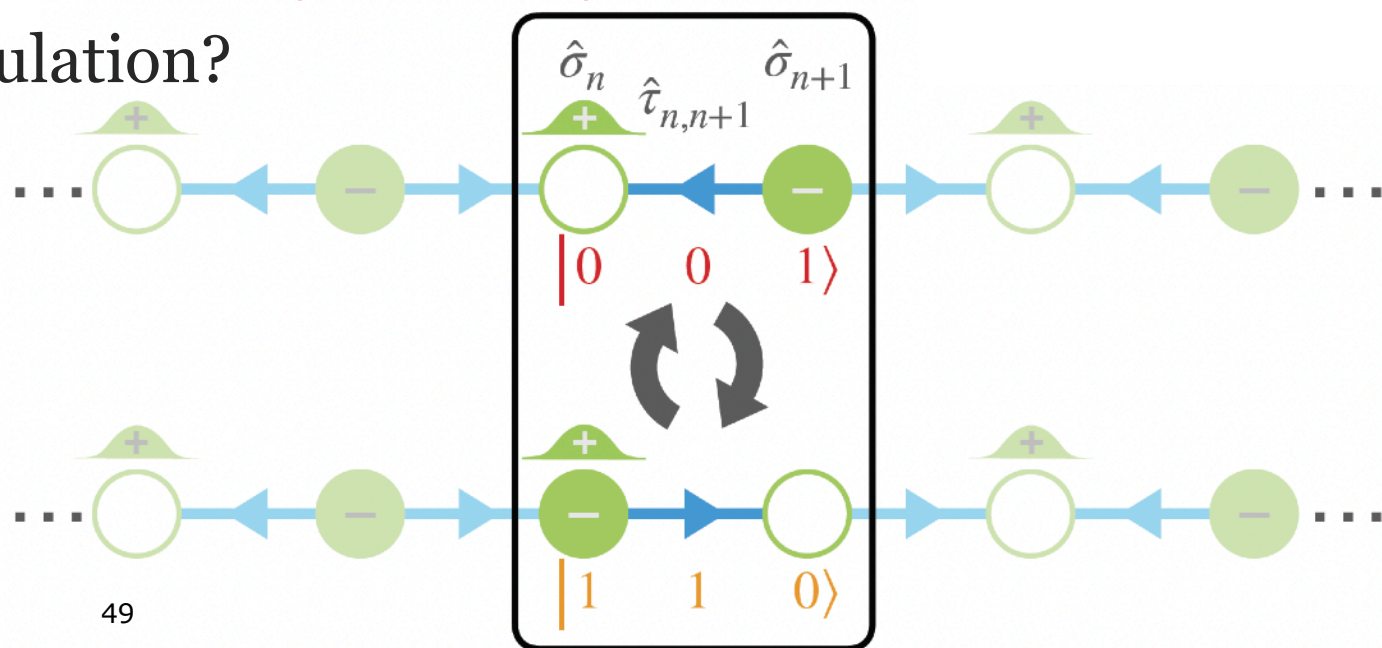
Banerjee et al., PRL 109, 175302 (2012)  
Yang et al., PRA 94, 052321 (2016)

# Matter-gauge interaction & Gauss's law

$$\text{Gauss's law } \hat{G}_n = \frac{1}{2}[\hat{\sigma}_n^z - (-1)^n] - \frac{1}{2}(\hat{\tau}_{n,n+1}^z - \hat{\tau}_{n-1,n}^z)$$

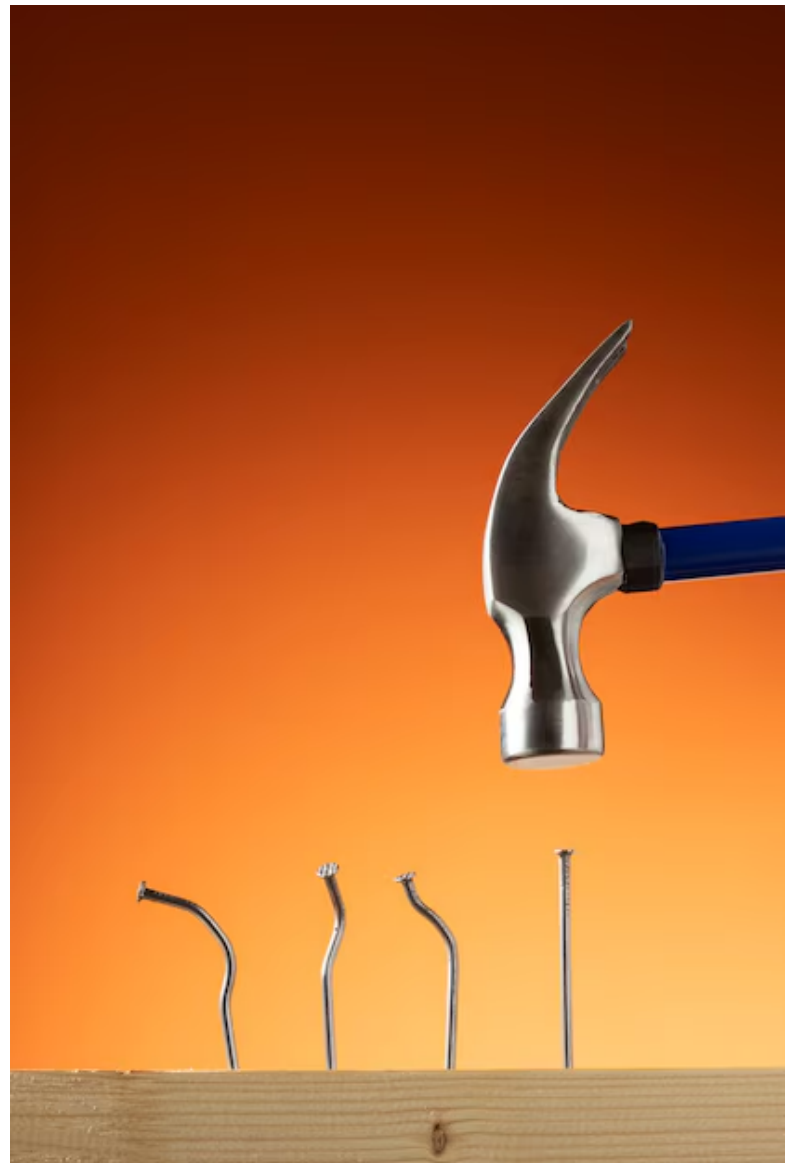
$$\hat{\mathcal{H}} = -J \sum_{n=1}^{L-1} (\hat{\sigma}_n^+ \hat{\tau}_{n,n+1}^+ \hat{\sigma}_{n+1}^- + \text{h.c.}) + \frac{\mu}{2} \sum_{n=1}^L (-1)^n \hat{\sigma}_n^z$$

- Charge hops across link while link flips:  $|001\rangle \leftrightarrow |110\rangle$
- How to realize this in quantum simulation?



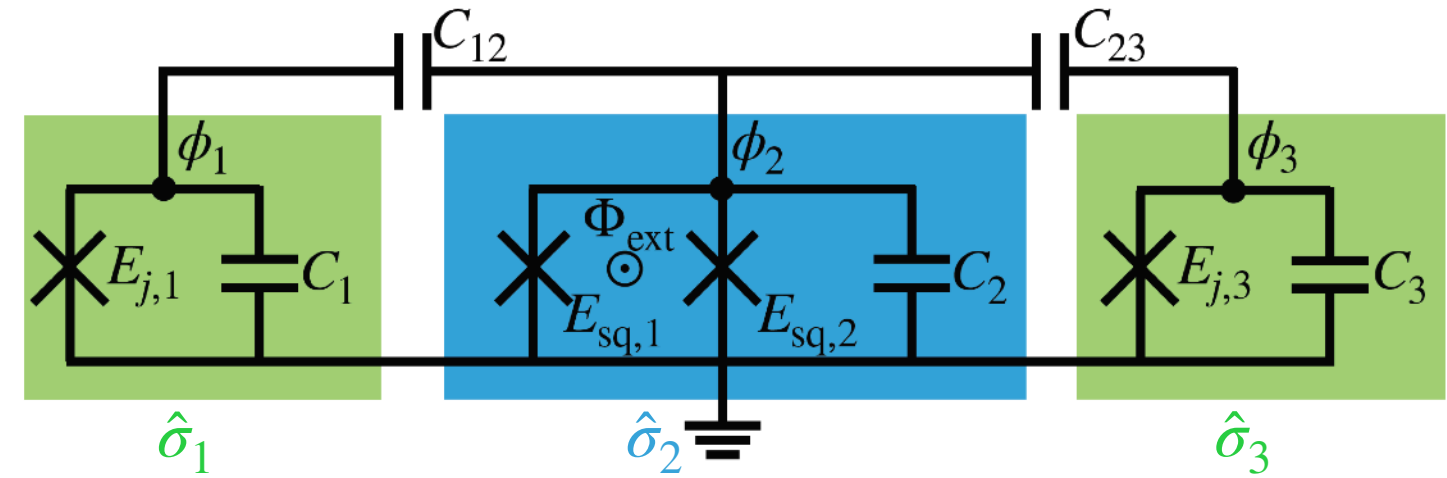
# Story so far

- We want to simulate transverse three-qubit interactions...
- ... and now we already know it is doable by parametric pumping!



# Device: three-qubit building block

- Three capacitively coupled transmon qubits

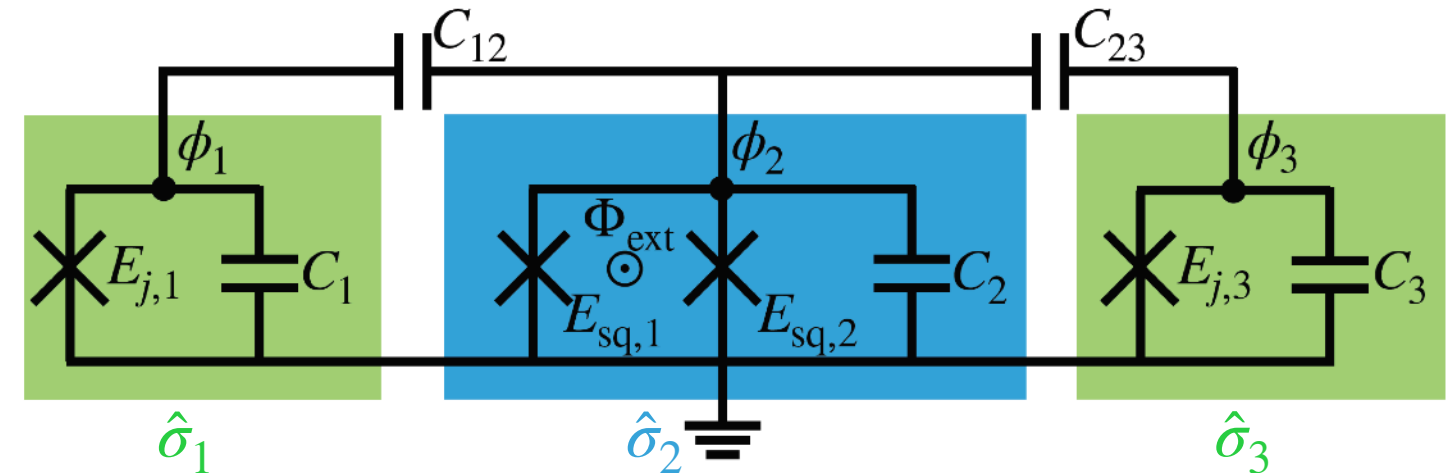


# Device: three-qubit building block

- Three capacitively coupled transmon qubits
  - Middle one tunable through *asymmetric* SQUID

- $$\hat{\mathcal{H}}_0 = \sum_{n=1}^3 \hbar\omega_n \frac{\hat{\sigma}_n^z + 1}{2} + \sum_{n=1}^2 \hbar\chi_{n,n+1} \frac{\hat{\sigma}_n^z + 1}{2} \frac{\hat{\sigma}_{n+1}^z + 1}{2}$$

Qubit freq.ZZ-coupling (cross-Kerr)



# Parametric toolbox: SQUID-mediated interactions

- **Asymmetric** SQUID:

$$\hat{H}_{\text{SQ}} = -E_J \cos \frac{\pi(\hat{\Phi}_p + \Phi_{\text{bias}})}{\Phi_0} \cos \hat{\phi}_2 + \delta E_J \sin \frac{\pi(\hat{\Phi}_p + \Phi_{\text{bias}})}{\Phi_0} \sin \hat{\phi}_2$$

Flux pump      SQUID phase

# Parametric toolbox: SQUID-mediated interactions

- **Asymmetric** SQUID:

$$\hat{H}_{\text{SQ}} = -E_J \cos \frac{\pi(\hat{\Phi}_p + \Phi_{\text{bias}})}{\Phi_0} \cos \hat{\phi}_2 + \delta E_J \sin \frac{\pi(\hat{\Phi}_p + \Phi_{\text{bias}})}{\Phi_0} \sin \hat{\phi}_2$$

Flux pump      SQUID phase

$$\hat{H}_{\text{SQ}} = \sum_k g_k(A_p) \left[ \sum_{n=1}^3 (\lambda_n \hat{\sigma}_n^+ + \lambda_n^* \hat{\sigma}_n^-) \right]^k$$

# Parametric toolbox: SQUID-mediated interactions

- **Asymmetric** SQUID:

$$\hat{H}_{\text{SQ}} = -E_{\text{J}} \cos \frac{\pi(\hat{\Phi}_p + \Phi_{\text{bias}})}{\Phi_0} \cos \hat{\phi}_2 + \delta E_{\text{J}} \sin \frac{\pi(\hat{\Phi}_p + \Phi_{\text{bias}})}{\Phi_0} \sin \hat{\phi}_2$$

Flux pump      SQUID phase

$$\hat{H}_{\text{SQ}} = \sum_k g_k(A_p) \left[ \sum_{n=1}^3 (\lambda_n \hat{\sigma}_n^+ + \lambda_n^* \hat{\sigma}_n^-) \right]^k$$

- Pump @  $\omega_p \approx (E_{110} - E_{001})/\hbar$ , where  $E_{110}/\hbar = \omega_1 + \omega_2 + \chi_{1,2}$ ,  $E_{001}/\hbar = \omega_3$
- Three-body interaction  $\propto -J(A_p) \hat{\sigma}_1^+ \hat{\sigma}_2^+ \hat{\sigma}_3^- + \text{h.c.}$ 
  - $k = 3$ , so **sine term is necessary**:  $J(A_p) \propto \delta E_{\text{J}} A_p$

Chang, ..., Wilson, PRX 10, 011011 (2020)  
Busnaina, ..., Wilson, in preparation

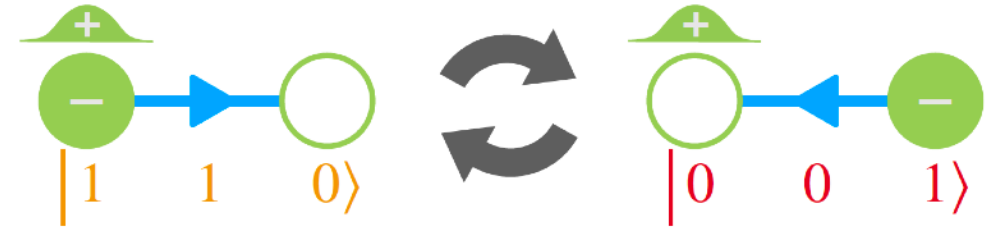
# Mapping to LGT Hamiltonian

- Three capacitively coupled transmon qubits
  - Pumping *asymmetric* SQUID of middle transmon

Busnaina, ..., Wilson, in preparation

# Mapping to LGT Hamiltonian

- Three capacitively coupled transmon qubits
  - Pumping *asymmetric* SQUID of middle transmon
  - Move to **gauge-invariant subspace**:  $|001\rangle$  &  $|110\rangle$
  - Rotating frame



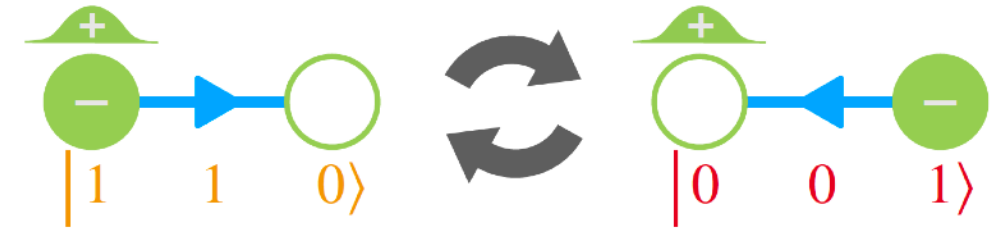
# Mapping to LGT Hamiltonian

- Three capacitively coupled transmon qubits
  - Pumping *asymmetric* SQUID of middle transmon
- Move to **gauge-invariant subspace**:  $|001\rangle$  &  $|110\rangle$
- Rotating frame

- $\hat{\mathcal{H}}_{\text{int}} = \frac{\mu(\omega_p)}{2} \sum_{n=1,2} (-1)^n \hat{\sigma}_n^z - J(A_p)(\hat{\sigma}_1^+ \hat{\tau}_{1,2}^+ \hat{\sigma}_2^- + \text{h.c.})$  where

$$\mu(\omega_p) = -[\hbar\omega_p - (E_{110} - E_{001})]/2$$

- Matter-gauge interaction strength  $\leftarrow$  pump strength
- Fermion mass  $\leftarrow$  pump detuning



Busnaina, ..., Wilson, in preparation

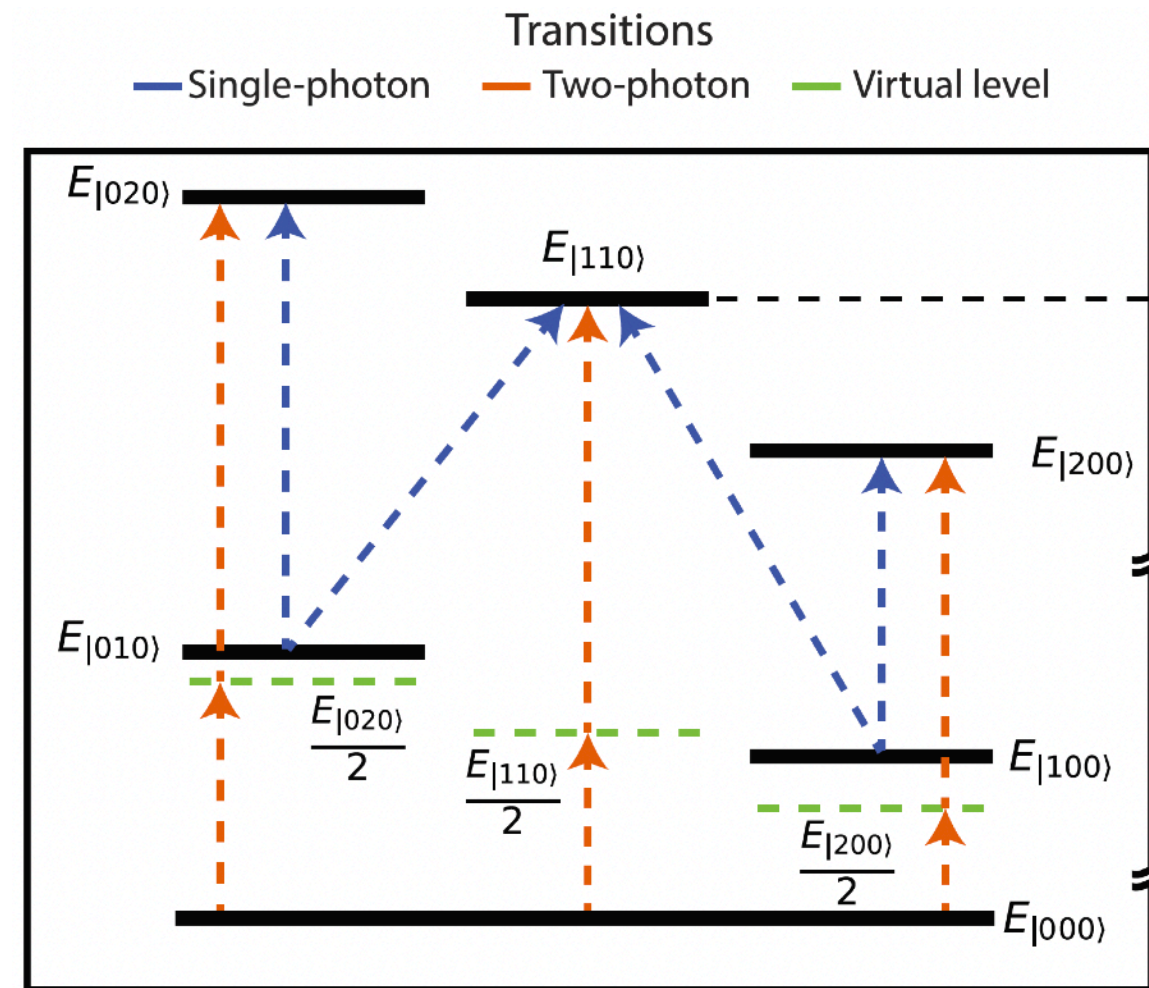
# Three-qubit interaction: state identification

- Experimentally, we must first find  $|110\rangle$ 
  - Not trivial because of strong coupling

Busnaina, ..., Wilson, in preparation

# Three-qubit interaction: state identification

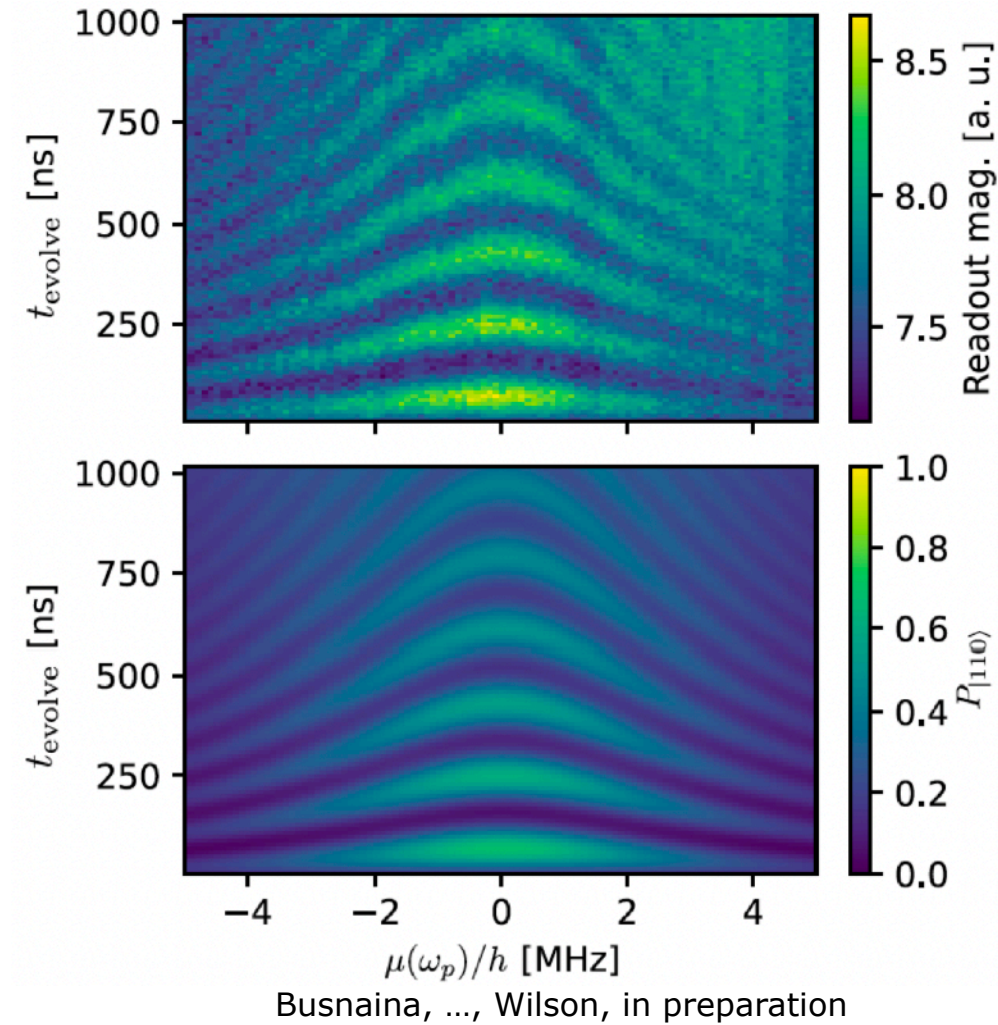
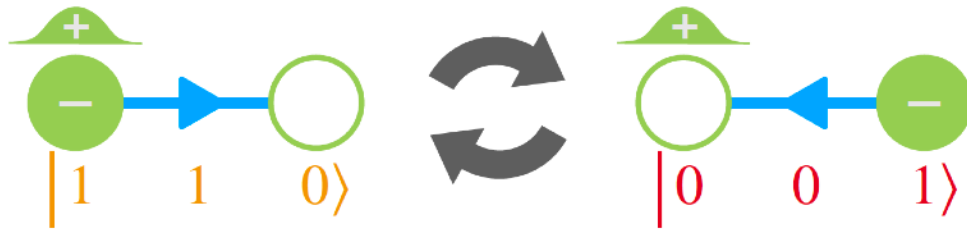
- Experimentally, we must first find  $|110\rangle$ 
  - Not trivial because of strong coupling
- Climb ladder of single-photon transitions:
  - $|000\rangle \rightarrow |100\rangle \rightarrow |200\rangle$  or  $|110\rangle$
  - $|000\rangle \rightarrow |010\rangle \rightarrow |020\rangle$  or  $|110\rangle$
- $|110\rangle$  is (by definition) the only two-photon state **accessible from both  $|100\rangle$  &  $|010\rangle$**



Busnaina, ..., Wilson, in preparation

# Three-qubit interaction: Rabi oscillations

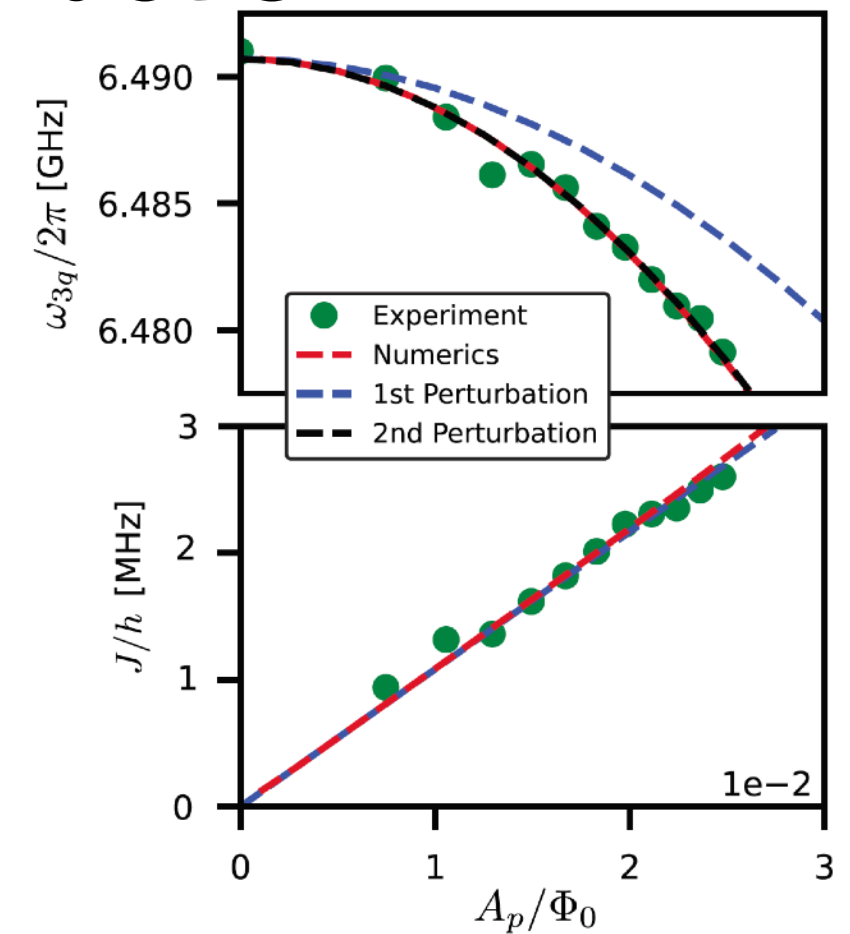
- Initialize in  $|001\rangle$
- Pump @  $\omega_p \approx (E_{110} - E_{001})/\hbar$  for time  $t_{\text{evolve}}$
- Rabi chevrons between  $|001\rangle$  &  $|110\rangle$



Busnaina, ..., Wilson, in preparation

# Characterizing three-qubit interaction

- $J(A_p) \propto \delta E_J A_p$ , as expected
- $|001\rangle - |110\rangle$  resonance freq.  $\omega_{3q}$  depends on  $A_p$  (ac Stark)
  - Two distinct  $O(A_p^2)$  contributions – adiabatic & nonadiabatic (Bloch-Siegert type)



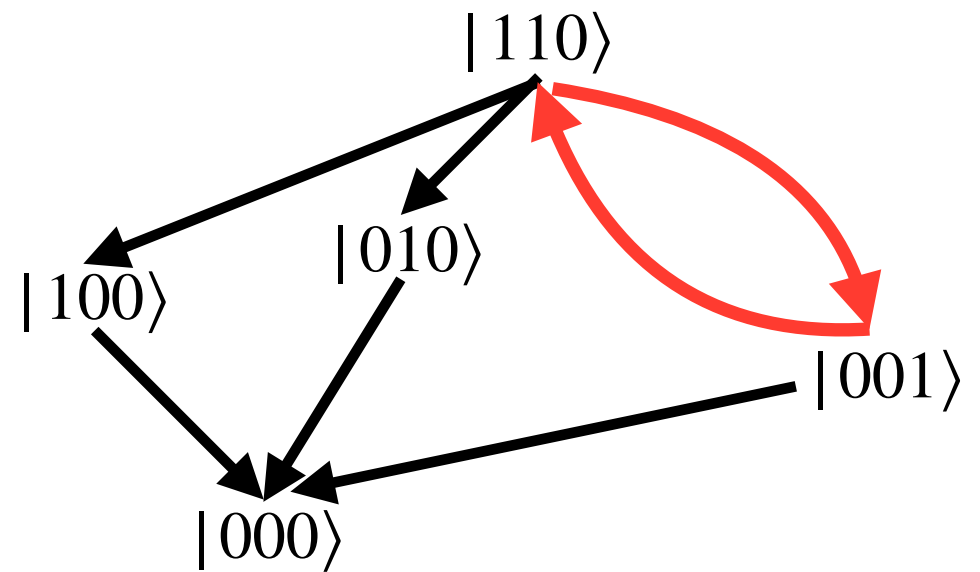
Noh et al., Nat. Phys. 19, 1445 (2023)  
Shirley, Phys. Rev. 138, B979 (1965)  
Busnaina, ..., Wilson, in preparation

# Dynamics of coupled qubit-resonator system

- Resonator decay time  $\sim$  qubit lifetime
  - How to “remove” resonators?

# Dynamics of coupled qubit-resonator system

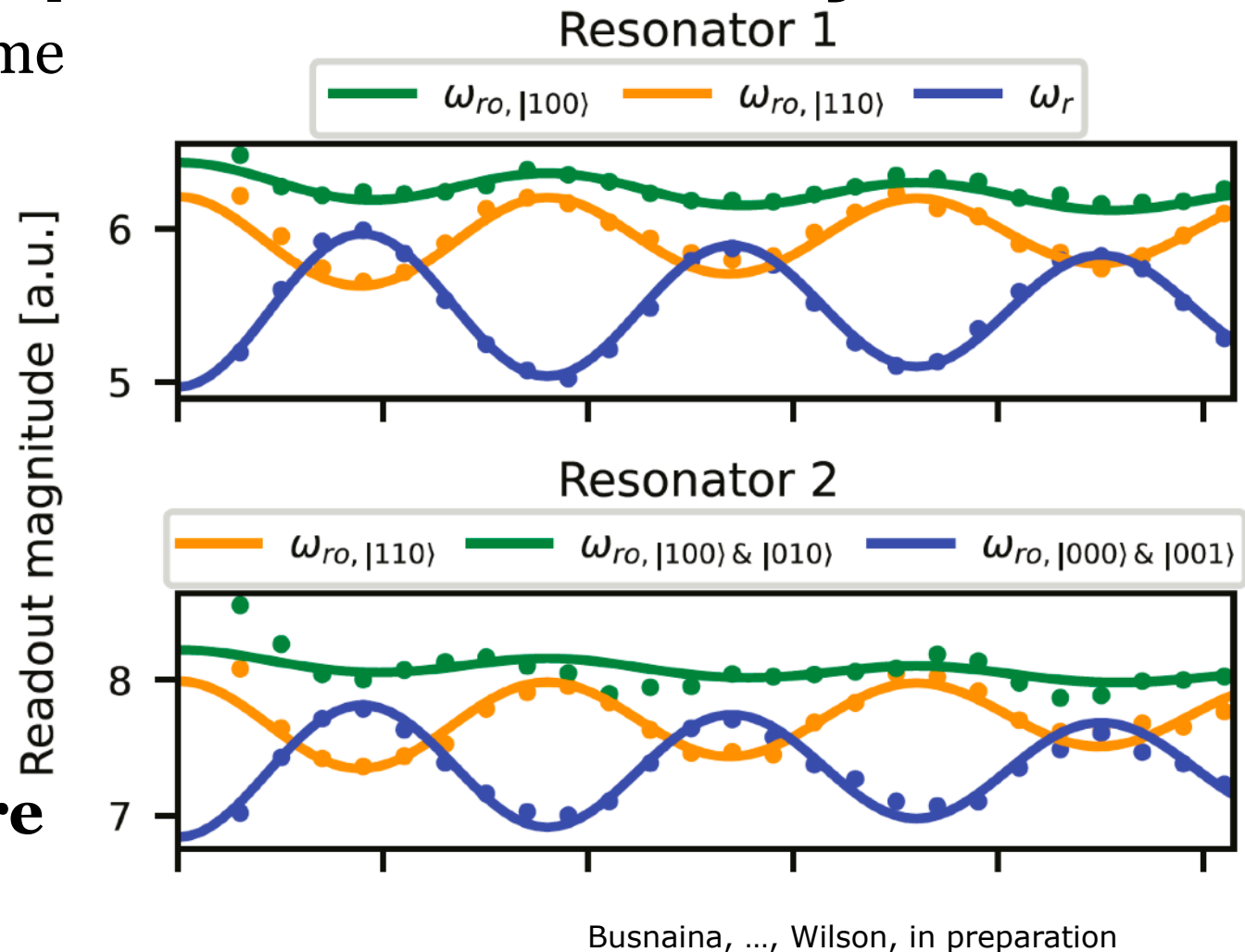
- Resonator decay time  $\sim$  qubit lifetime
  - How to “remove” resonators?
- Simplified model:  $|001\rangle, |110\rangle, |100\rangle, |010\rangle, |000\rangle$  + resonator



Busnaina, ..., Wilson, in preparation

# Dynamics of coupled qubit-resonator system

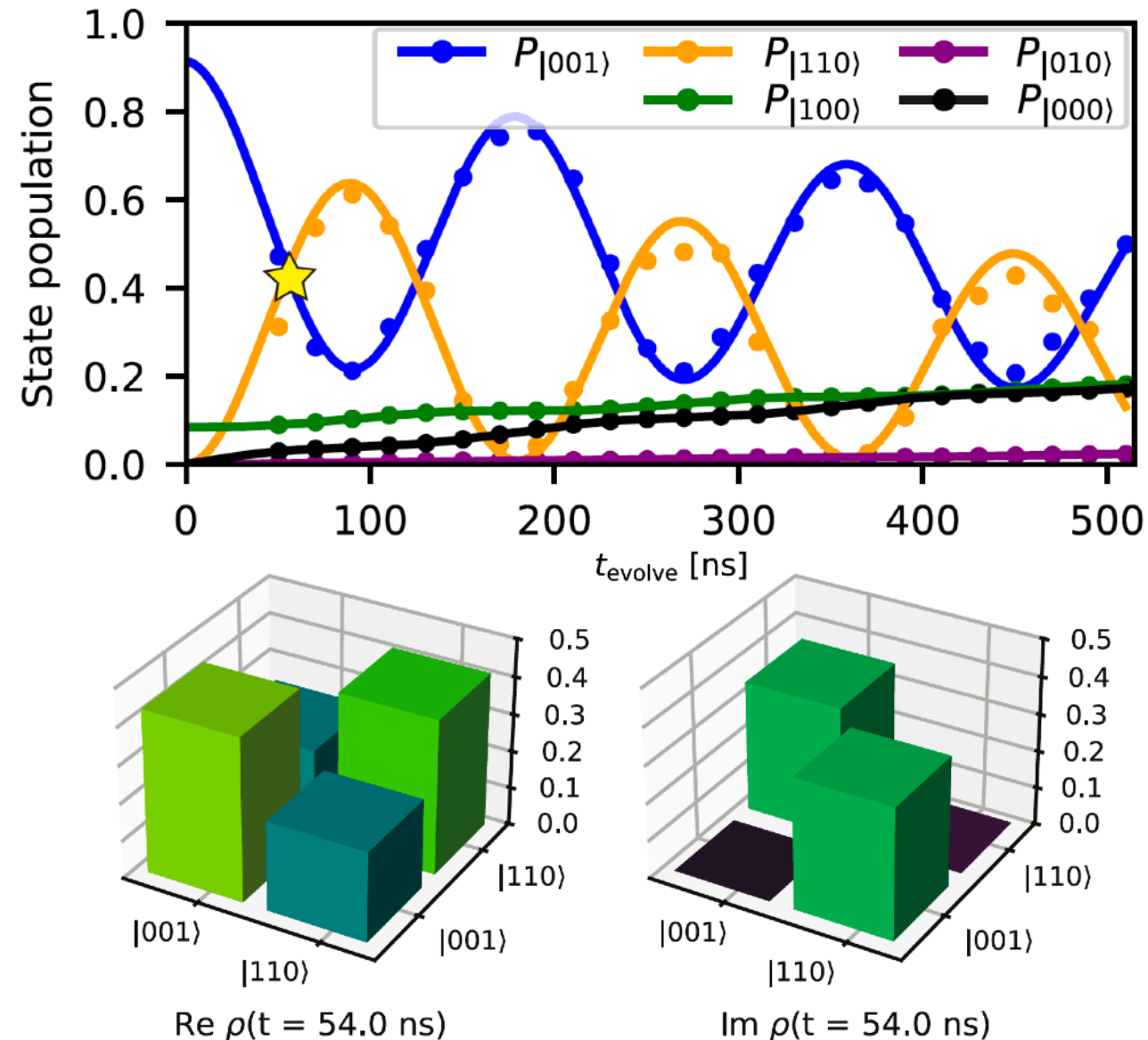
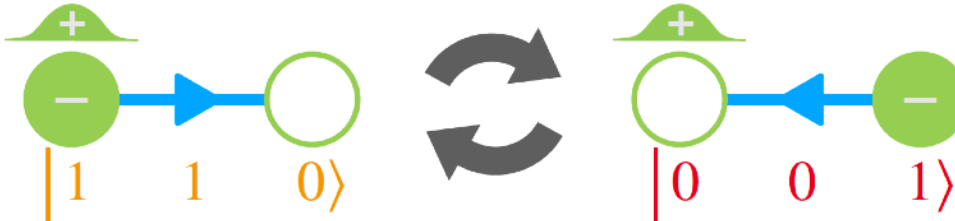
- Resonator decay time  $\sim$  qubit lifetime
  - How to “remove” resonators?
- Simplified model:  $|001\rangle, |110\rangle, |100\rangle, |010\rangle, |000\rangle$  + resonator
- Readout @ different freq.
  - Fit to coupled EoM (“cavity-Bloch”) to determine qubit state population **immediately before readout**



Busnaina, ..., Wilson, in preparation

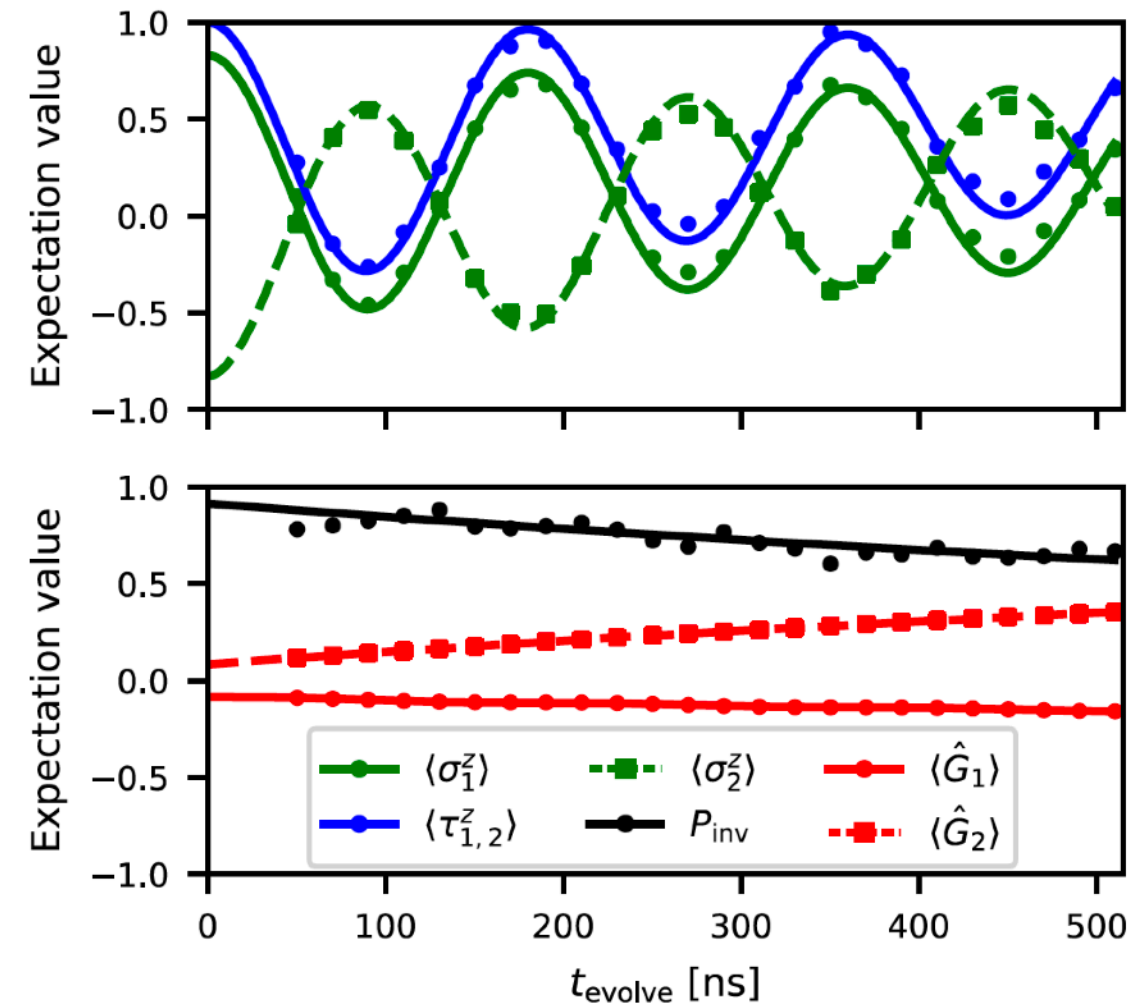
# State populations

- Oscillations in extracted populations  $|001\rangle$  &  $|110\rangle$
- At  $t = 54$  ns (star), extracted density matrix shows coherent superposition of  $|001\rangle$  &  $|110\rangle$



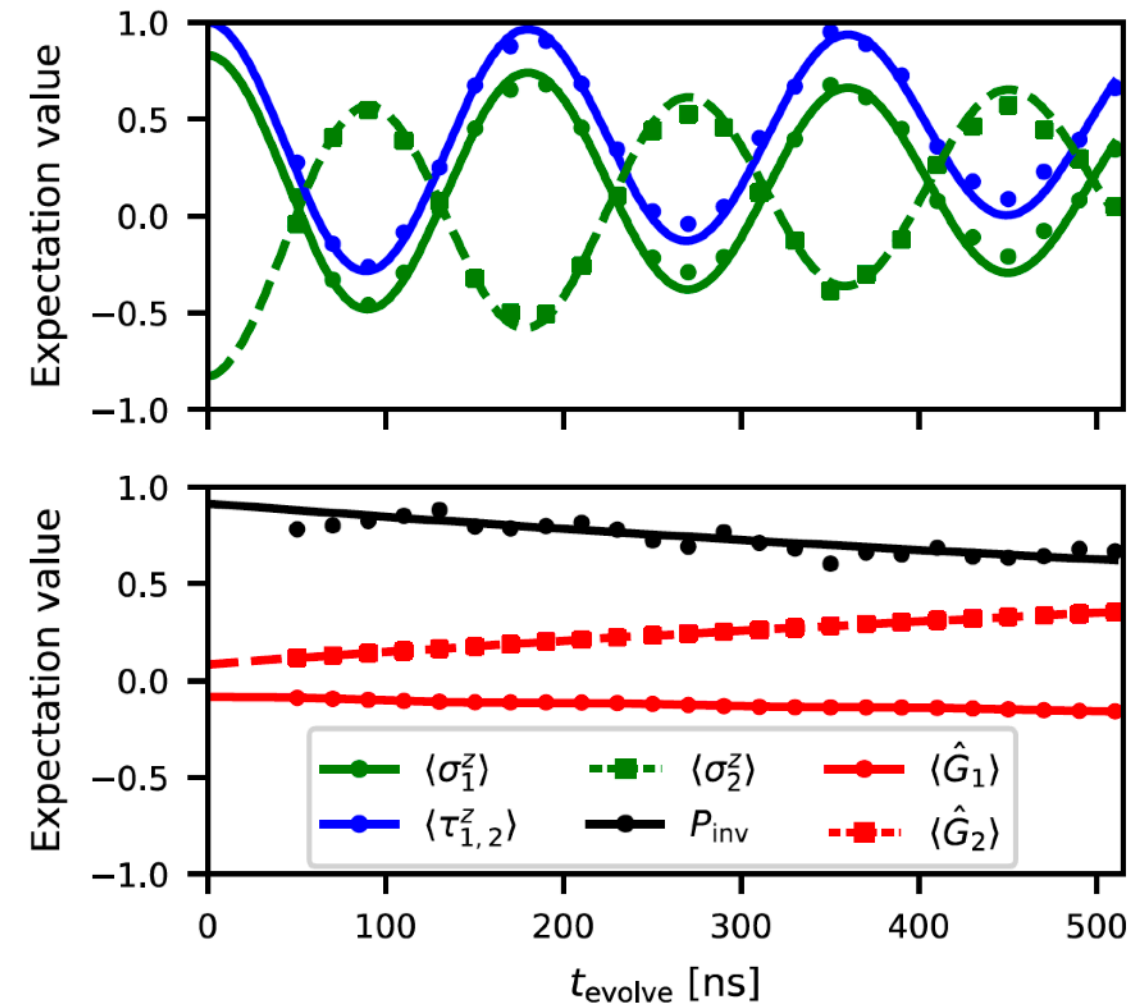
# Expectation values & Gauss's law

- Oscillations in all spin expectation values  $\langle \hat{\sigma}_1^z \rangle$ ,  $\langle \hat{\tau}_{1,2}^z \rangle$  &  $\langle \hat{\sigma}_2^z \rangle$
- Suppressed oscillations in gauge-invariant sector population,  
 $P_{\text{inv}} = P_{|110\rangle} + P_{|001\rangle}$



# Expectation values & Gauss's law

- Oscillations in all spin expectation values  $\langle \hat{\sigma}_1^z \rangle$ ,  $\langle \hat{\tau}_{1,2}^z \rangle$  &  $\langle \hat{\sigma}_2^z \rangle$
- Suppressed oscillations in gauge-invariant sector population,  
 $P_{\text{inv}} = P_{|110\rangle} + P_{|001\rangle}$ 
  - Slow leakage out of gauge-invariant subspace
  - **Gauss's law satisfied within qubit lifetime**



# Conclusion II: 3-qubit interaction & LGT

- Building block for LGT simulation with three-qubit interaction
- Interaction **preserves Gauss's law**

Busnaina, ZS, Alcaine-Cuervo, Yang, Nsanzineza, Rico & Wilson  
in preparation

# Conclusion II: 3-qubit interaction & LGT

- Building block for LGT simulation with three-qubit interaction
- Interaction **preserves Gauss's law**
- Reduces overhead due to decomposing into single- & two-qubit gates
- Outlook
  - More complicated dynamical gauge fields (higher spin,  $SU(2)$ , ...)
  - Scaling up!

Busnaina, ZS, Alcaine-Cuervo, Yang, Nsanzineza, Rico & Wilson  
in preparation



UNIVERSITÉ DE  
SHERBROOKE



CANADA  
FIRST  
RESEARCH  
EXCELLENCE  
FUND



Innovation, Science and  
Economic Development Canada

APOGÉE  
CANADA  
FONDS  
D'EXCELLENCE  
EN RECHERCHE



Universidad  
del País Vasco



THE UNIVERSITY OF  
CHICAGO

INNOVATION

Canada Foundation  
for Innovation

Fondation canadienne  
pour l'innovation



MINISTRY OF  
RESEARCH AND INNOVATION

# Thank you!

Jamal Busnaina, Dmytro Dubyna, Cindy Yang,

Ibrahim Nsanzineza, Jimmy Hung, Sandbo Chang, **Chris Wilson**

Alexander McDonald, Jesús Alcaine-Cuervo, Aashish Clerk, Enrique Rico



UNIVERSITY OF  
WATERLOO



**NSERC**  
**CRSNG**

**IQC** Institute for  
Quantum  
Computing

$$\dot{\hat{x}}_j = \frac{1}{2\hbar} \left[ (t \sin \varphi_t + \Delta) \hat{x}_{j-1} - (t \sin \varphi_t - \Delta) \hat{x}_{j+1} + t \cos \varphi_t (\hat{p}_{j-1} + \hat{p}_{j+1}) \right], \quad (2)$$

$$\dot{\hat{p}}_j = \frac{1}{2\hbar} \left[ (t \sin \varphi_t - \Delta) \hat{p}_{j-1} - (t \sin \varphi_t + \Delta) \hat{p}_{j+1} - t \cos \varphi_t (\hat{x}_{j-1} + \hat{x}_{j+1}) \right]. \quad (3)$$

$$E_n^0 = \sqrt{t^2 - \Delta^2} \cos k_n - i \frac{\kappa}{2},$$

$$E_n^p = t \sin \varphi_t \sin k_n \pm i \sqrt{\Delta^2 - t^2 \cos^2 \varphi_t} \cos k_n - i \frac{\kappa}{2},$$

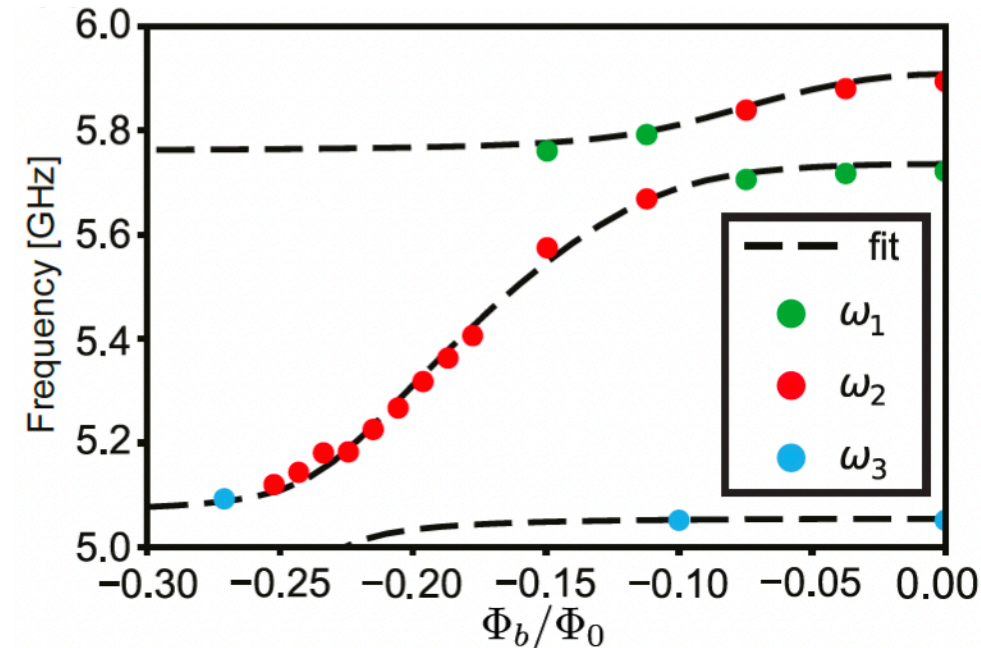
$$\hat{d}_n \propto \sum_j \sin(k_n j) (e^{rj} \hat{x}'_j + i e^{-rj} \hat{p}'_j), e^{-2r} = \frac{|t' - \Delta'|}{t' + \Delta'},$$

$$\hat{\mathcal{H}}_S = \sum_j \hbar \delta \omega_j \hat{a}_j^\dagger \hat{a}_j + \frac{1}{2} \sum_{\langle jj' \rangle} \left( t_{jj'} e^{i\varphi_{jj'}^t} \hat{a}_j^\dagger \hat{a}_{j'} + \Delta_{jj'} e^{i\varphi_{jj'}^\Delta} \hat{a}_j \hat{a}_{j'} + \text{h.c.} \right).$$

# Device characterization

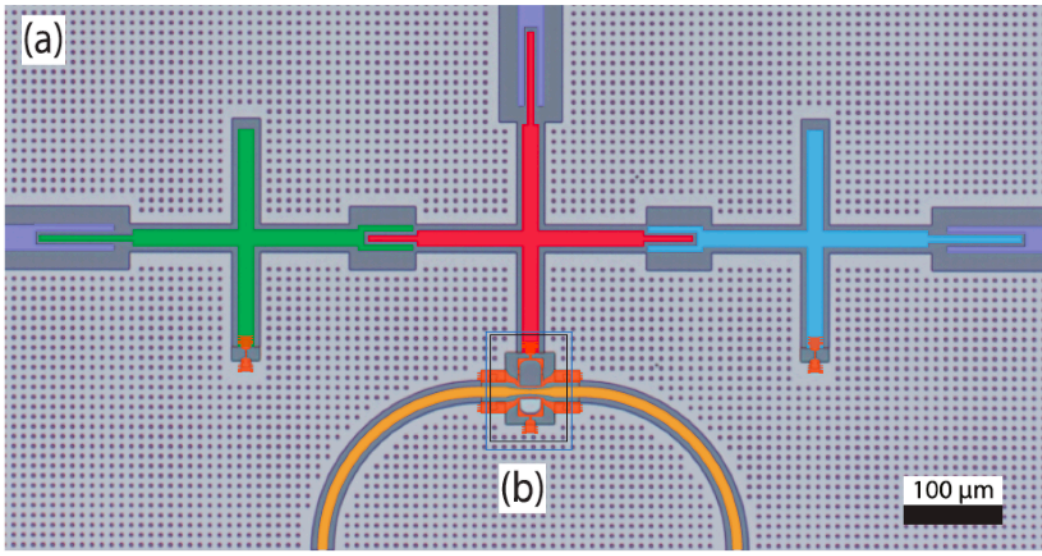
Fit circuit model to:

- Qubit freq. vs dc flux bias
- @ zero dc flux bias:
  - Two-photon energy levels
  - Three-body interaction vs ac flux drive

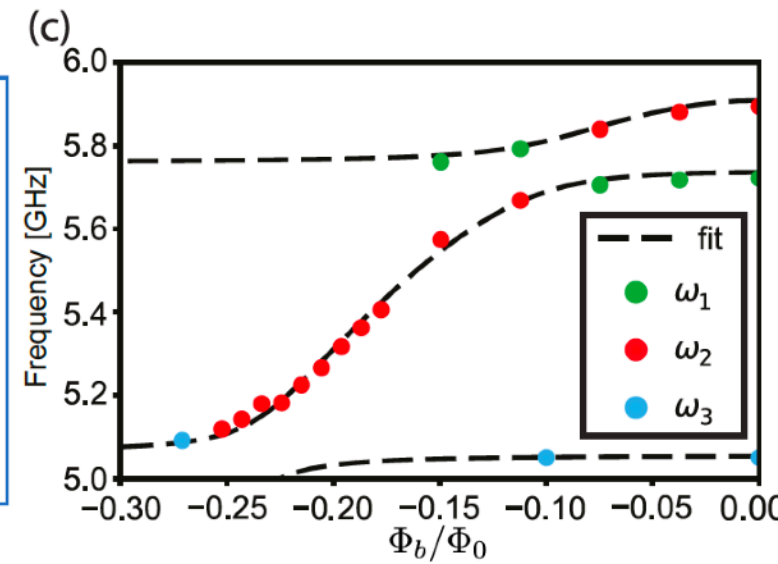
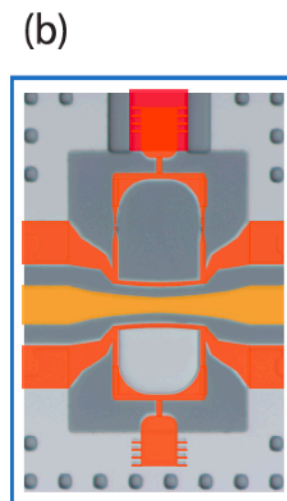


Qubit	1	2	3
$\omega_n/2\pi$ [GHz]	5.725	5.910	5.055
$(E_C/\hbar)/2\pi$ [MHz]	183	165	184
Qubits $n-m$	1-2	1-3	2-3
$(g_{nm}/\hbar)/2\pi$ [MHz]	63	18	108

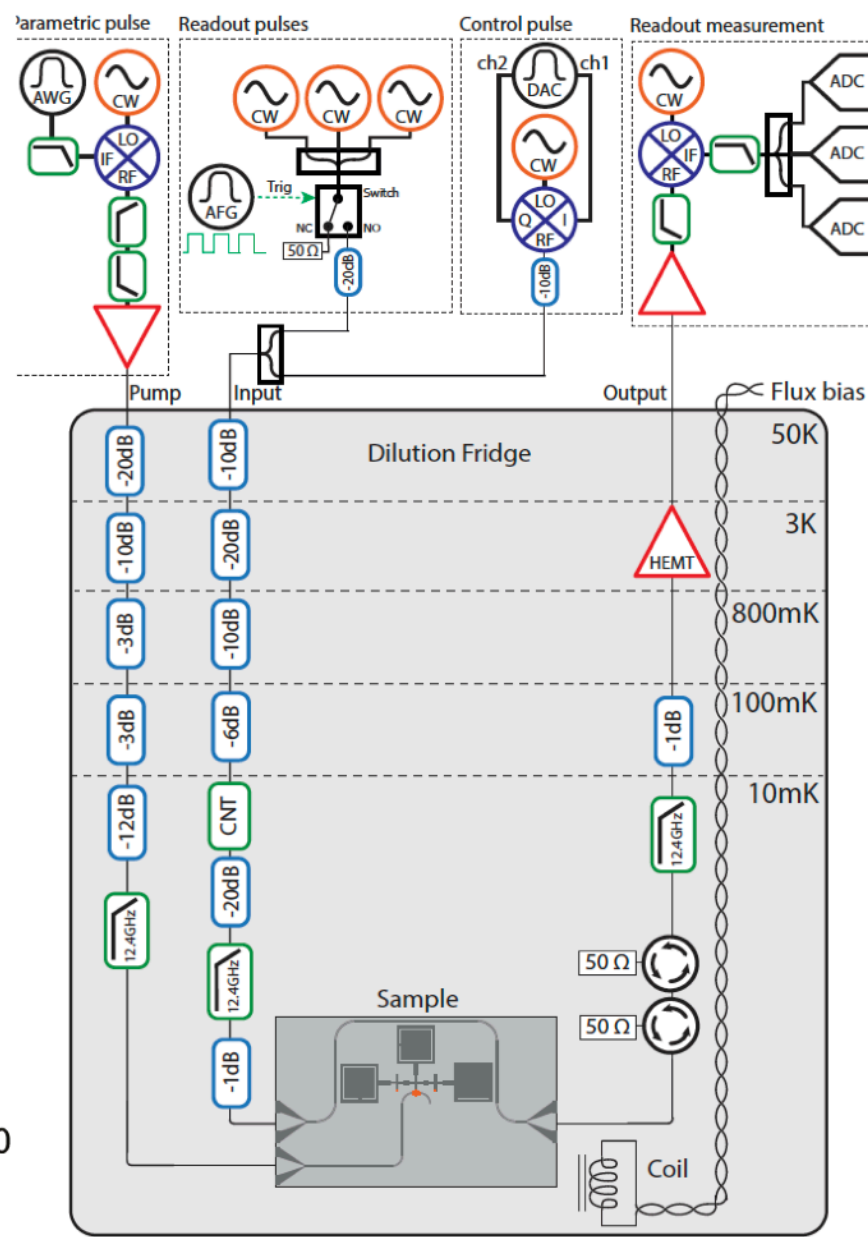
Busnaina, ..., Wilson, in preparation



■ Qubit 1 ■ Qubit 2 ■ Qubit 3 ■ Resonators ■ AC flux



Analog quantum simulation of bosonic lattices and lattice gauge theories



Readout resonator	1	2	3
$\omega_r/2\pi$ [GHz]	7.698	7.518	7.035
$\kappa_{\text{int}}/2\pi$ [MHz]	0.439	0.489	5.1
$\kappa/2\pi$ [MHz]	0.650	0.643	6.37
$\eta$	0.325	0.240	0.199

TABLE III. Resonator parameters extracted from VNA measurements, including resonance frequencies, internal and external decay rates.

Qubit	1	2	3
$\omega_q/2\pi$ [GHz]	5.725	5.910	5.055
$T_1$ [ns]	4216	1302	$4152 \pm 2426$
$T_{\text{Ramsey}}$ [ns]	2470	971	2907
$T_{\text{Echo}}$ [ns]	-	965	4527
$2\chi^{R1}/2\pi$ [MHz]	-7.3	-0.4	0
$2\chi^{R2}/2\pi$ [MHz]	-2.2	-2.4	0
$2\chi^{R3}/2\pi$ [MHz]	-2	-3	-0.5

TABLE IV. Qubit frequencies, anharmonicities, lifetimes, and dispersive shifts of resonator frequencies extracted during device characterization.

$$\begin{aligned}\hat{H}_{\text{cB}}/\hbar = & (\omega_r + 2 \sum_s \chi_s |s\rangle \langle s|) \hat{a}^\dagger \hat{a} \\ & + \alpha \hat{a}^\dagger \hat{a}^\dagger \hat{a} \hat{a} + \sum_s \omega_s |s\rangle \langle s| \\ & + (\epsilon_m(t) \hat{a}^\dagger e^{-i\omega_m t} + \epsilon_m^*(t) \hat{a} e^{i\omega_m t}) \\ & + (\Omega(t) |110\rangle \langle 001| e^{-i\omega_p t} \\ & + \Omega^*(t) |001\rangle \langle 110| e^{i\omega_p t}),\end{aligned}$$

$$\begin{aligned}\frac{d}{dt} \langle |001\rangle \langle 001| \hat{a} \rangle \\ = & -i [\Omega^*(t) \langle |001\rangle \langle 110| \hat{a} \rangle - \Omega(t) \langle |110\rangle \langle 001| \hat{a} \rangle] \\ & - (\gamma_{001 \rightarrow 000} + \frac{\kappa}{2}) \langle |001\rangle \langle 001| \hat{a} \rangle \\ & + \gamma_{000 \rightarrow 001} \langle |000\rangle \langle 000| \hat{a} \rangle \\ & - i (\omega_r - \omega_m + 2\alpha \langle \hat{a}^\dagger \hat{a} \rangle + 2\chi_{001}) \langle |001\rangle \langle 001| \hat{a} \rangle \\ & - i\epsilon_m(t) \langle |001\rangle \langle 001| \rangle,\end{aligned}$$

$$\begin{aligned}\frac{d}{dt} \langle |001\rangle \langle 001| \rangle \\ = & -i [\Omega^*(t) \langle |001\rangle \langle 110| \rangle - \Omega(t) \langle |110\rangle \langle 001| \rangle] \\ & - \gamma_{001 \rightarrow 000} \langle |001\rangle \langle 001| \rangle + \gamma_{000 \rightarrow 001} \langle |000\rangle \langle 000| \rangle, \\ \frac{d}{dt} \langle |110\rangle \langle 110| \rangle \\ = & i [\Omega^*(t) \langle |001\rangle \langle 110| \rangle - \Omega(t) \langle |110\rangle \langle 001| \rangle] \\ & - (\gamma_{110 \rightarrow 100} + \gamma_{110 \rightarrow 010}) \langle |110\rangle \langle 110| \rangle \\ & + \gamma_{100 \rightarrow 110} \langle |100\rangle \langle 100| \rangle + \gamma_{010 \rightarrow 110} \langle |010\rangle \langle 010| \rangle, \\ \frac{d}{dt} \langle |100\rangle \langle 100| \rangle \\ = & -(\gamma_{100 \rightarrow 000} + \gamma_{100 \rightarrow 110}) \langle |100\rangle \langle 100| \rangle \\ & + \gamma_{110 \rightarrow 100} \langle |110\rangle \langle 110| \rangle + \gamma_{000 \rightarrow 100} \langle |000\rangle \langle 000| \rangle,\end{aligned}$$

